Instability of nonlinear Trivelpiece-Gould waves I: Wave degeneracies

Cite as: Phys. Plasmas **26**, 102111 (2019); https://doi.org/10.1063/1.5116375
Submitted: 24 June 2019 . Accepted: 19 September 2019 . Published Online: 15 October 2019

Daniel H. E. Dubin

Physics of Plasmas ARTICLE scitation.org/journal/php

Instability of nonlinear Trivelpiece-Gould waves I: Wave degeneracies

Cite as: Phys. Plasmas **26**, 102111 (2019); doi: 10.1063/1.5116375
Submitted: 24 June 2019 · Accepted: 19 September 2019 ·
Published Online: 15 October 2019

Daniel H. E. Dubin

AFFILIATIONS

Department of Physics, UCSD, La Jolla, California 92093, USA

ABSTRACT

Arguments based on energy conservation are used to evaluate the fluid theory of stability of nonlinear traveling waves (pump waves) in an ideal plasma system. Instabilities growing on the pump wave are associated with wave degeneracies. The relative signs of the energies of degenerate waves, as seen in the frame of the pump wave, determine whether their amplitudes grow exponentially or merely oscillate through resonant energy exchange. This energy analysis is carried out in detail for Trivelpiece-Gould (TG) waves and is compared to numerical calculations. It is verified that nonlinear TG waves are stable with respect to 3 wave processes, but weaker 4 wave, 5 wave, and higher order wave processes cause instability over narrow wavenumber bands. A modulational instability is also identified.

I. INTRODUCTION

In this paper, we consider stability with respect to small perturbations of finite amplitude traveling waves (pump waves) in an ideal (i.e., dissipationless) fluid. This is a subject that has received considerable attention in several fields of physics. A range of theoretical approaches have been applied to the problem, with results growing up around seemingly disparate instability mechanisms such as parametric decay instability, modulational instability, and more general 3-wave, 4-wave, and even higher-order multiwave processes.

For example, in fluid mechanics, the stability of cnoidal waves in shallow water, and of Stokes waves in deeper water, is quite well developed.[1–7] The theory of modulational instability benefited greatly from wave-averaged Lagrangian techniques developed over this period.[8,9] Higher order resonant processes leading to instability were also uncovered.[10,11] In plasma physics, early theory work described parametric and modulational processes, leading to instability in various nonlinear plasma waves.[12–14] Many such plasma instabilities have been studied over the years[15–20] in relation to fusion plasmas, astrophysical plasmas, and laser-plasma interactions.

The nonlinear stability of waves is often described in terms of multiwave processes. For a 3-wave process on a nonlinear wave, three interacting waves, one of which is the nonlinear pump wave, satisfy resonance conditions for both the frequency and wavenumber, which allow resonant energy and momentum exchange, leading to decay of the pump wave amplitude and exponential growth of the other two waves (termed daughter waves)

$$\omega_1 = \omega_2 + \omega_3,$$
$$k_1 = k_2 + k_3. \quad (1)$$

These resonance conditions can be justified using arguments based on energy and momentum conservation in the exchange of wave quanta.[12] The instability growth rate is then typically connected via a two-time scale analysis to the theory of resonance in the parametric oscillator[12] or the Van der Pol equation.[13] For a higher-order "p-wave" process such as modulational instability (a 4-wave process), p waves are involved in the two resonance conditions.

In this paper, we employ a somewhat different approach, along the lines of arguments based on energy conservation.[21,22] There is a long history of using energy arguments in understanding plasma and fluid stability.[23–25] For our purposes, the general idea is accessibly discussed in broad terms in Ref. 26. We take advantage of the following observation: in the frame of an isolated pump wave, the fluid is a time-independent flow. This implies that the energy of small perturbations to the flow, when viewed in this stationary wave frame, is a conserved quantity (in the idealized dissipationless limit). By considering this energy, we are able to formulate a unified picture of the fluid instabilities on a pump wave: parametric, modulational, or other multiwave instabilities are all the result of a resonant interaction (degeneracy) between two daughter waves. Because the frequency of the pump wave is zero in the wave frame, and only the pump is treated as being nonlinear, the resonance conditions for a p wave process, with $p \equiv |m| + 2$ (m an integer), simplify to

$$\omega_1 = \omega_2,$$
$$k_1 = k_2 + mk_f, \tag{2}$$

where $k_f > 0$ is the fundamental wavenumber of the pump wave and subscripts 1 and 2 label wavenumbers and frequencies in each daughter wave [which may be positive or negative, indicating the sign (direction) of the wave phase velocities]. In this picture, however, the daughter waves are not single spatial Fourier modes, except at very small pump wave amplitudes. The daughter waves generally consist of many spatial Fourier harmonics due to the spatial nonuniformity of the plasma caused by the pump wave. However, all harmonics are separated by multiples of the pump wavenumber k_f, because the pump wave modulates the plasma at this wavenumber and its harmonics. The condition on wavenumbers in Eq. (2) then implies that the spatial Fourier harmonics of the two daughter waves occur for the same set of wavenumbers, albeit with different amplitudes and phases. Thus, labeling an instability as a p-wave process is rigorous only at small pump amplitudes, where the daughter waves are nearly single Fourier modes. However, we find that our numerical solutions for instability growth rates are well described by our small amplitude theory expressions involving p-wave processes, even at quite large amplitudes.

It is well known that the term mk_f in Eq. (2) arises from various types of mode coupling between the daughter waves and the pump wave. For example, the nonlinearity in the fluid equations directly couples two daughter wave Fourier amplitudes through the *mth* Fourier harmonic of the nonlinear pump wave. Another process couples the m–1st pump wave harmonic to a daughter wave harmonic, producing a perturbation that then couples the first harmonic of the pump to the second daughter wave and so on. For small pump amplitudes, these processes can be elegantly analyzed using $|m|$th-order degenerate perturbation theory for the resonant daughter waves, rather than through high-order two-time scale analysis or wave-averaged Lagrangians. For larger amplitudes, we solve for the full spectrum of linear daughter wave perturbations using a numerical method based on the Hills method.[27]

However, the satisfaction of the resonance conditions (2) does not necessarily cause instability of the pump wave. This is, perhaps, not well known. The energy approach to instability provides an extra insight, leading to a simple and general instability condition.[21,22,26] If the energies of the resonant daughter waves (as seen in the moving frame of the pump wave) are of the same sign, their resonant interaction leads only to a frequency shift with no instability (this is the case of an "avoided crossing" in degenerate perturbation theory). However, if the daughter wave energies are of *opposite sign*, then instability can occur. Physically, the negative energy daughter wave resonantly transfers energy to the positive energy daughter wave, allowing the positive energy wave to grow. As the energy of the negative energy wave decreases in this transfer, its amplitude *also increases*, allowing both waves to grow exponentially in a feedback loop. (If the energy transfer is in the opposite direction, the daughter waves are instead exponentially damped. The direction of energy transfer depends on the relative phase of the daughter waves, and a general initial condition can be decomposed into both a growing and a damped response.) Under more general conditions where the daughter waves and the pump have similar initial amplitudes, "explosive" instability leading to finite-time singularity can occur if two of the waves have energies of opposite signs.[13] In our analysis, the daughter waves are treated as linear perturbations of the finite-amplitude pump, so the instability is exponential, not explosive.

We carry out the energy analysis in detail for a particular system, nonlinear Trivelpiece–Gould (TG) plasma waves in one spatial dimension, in order to make contact with some past and current experiments.[28,29] However, the wave energy formalism is general and can be applied to a range of ideal fluid traveling waves.[26] Using this approach, we are able to derive analytic expressions for the growth rate of the fluid instabilities on the pump wave. We compare these theory predictions to numerical evaluations of the spectrum of perturbations on a pump wave. A previously undescribed modulational instability of the TG system is found, which has properties similar to the analogous instability observed in Stokes waves.[7] Weak instabilities associated p-wave processes with $p \geq 4$ are also found, over narrow wavenumber bands for the daughter waves.

The energy approach to instability can also be fruitfully applied to analyze other nonlinear wave effects, the theory of which cannot be included in this paper (mainly for the sake of brevity), such as convective vs absolute instability associated with plasma inhomogeneity and finite wavetrain length, nonlinear evolution of instability, weak or strong wave turbulence, or the effects of wave-particle interactions. Wave-particle interactions, and in particular, a new mechanism for parametric decay due to trapped particles,[29,30] will be considered in the following paper.[42]

In Sec. II, we briefly review the theory of nonlinear TG waves. In Sec. III, the stability of these waves is considered, and in Sec. IV, conclusions and open questions are discussed. Appendix A contains details of the degenerate perturbation theory used in the stability analysis.

II. NONLINEAR TRAVELING WAVES

Trivelpiece-Gould waves are electrostatic compressional plasma waves, excited in a cylindrical plasma column to which a confining magnetic field has been applied along the direction of the column axis (taken here to be the z direction).[31,32] Here, we consider the linear stability of finite-amplitude cylindrically symmetric traveling wave solutions (pump waves) propagating in one-dimension z, which are periodic in z, with fundamental wave period λ_f. While the pump waves are periodic with period λ_f, perturbations on the pump wave are assumed to be periodic with period $M\lambda_f$, for any positive integer value of M. The case $M = 2$ was covered in a previous publication,[33] but here we consider all values of M in order to search for more general instabilities.

As discussed in previous publications,[33,34] cylindrically symmetric TG waves that are without radial nodes can be approximately described by a coupled set of three partial differential equations in z and time t which evolve the plasma density $N(z, t)$, the fluid velocity $V(z,t)$, and the plasma potential $\Phi(z,t)$. These functions have been averaged radially over the plasma column to remove the radial dependence and simplify the theory.

Throughout this paper, we work in scaled units, with distances scaled to the fundamental wavenumber $k_f = 2\pi/\lambda_f$ of the pump wave, density scaled to the equilibrium density n_0, times scaled to the plasma frequency $\omega_p = \sqrt{4\pi e^2 n_0/m_p}$, velocity scaled to ω_p/k_f, and potential scaled to $(m_p/e)\omega_p^2/k_f^2$, where m_p and e are particle mass and charge, respectively. In these units, the governing equations are the scaled continuity, momentum, and Poisson equations

$$\frac{\partial N}{\partial t}+\frac{\partial}{\partial z}(\mathrm{V}N)=0,$$
$$\frac{\partial \mathrm{V}}{\partial t}+\frac{\partial}{\partial z}\left(\frac{1}{2}\mathrm{V}^2+\Phi\right)=0,$$
$$\frac{\partial^2\Phi}{\partial z^2}-k_\perp^2\Phi=-N+1. \tag{3}$$

Here, $k_\perp$ is a dimensionless parameter, the scaled perpendicular wavenumber for the waves, determined in experiments by the plasma radius r_p and the radius r_c of the surrounding confinement electrode, with $k_\perp \approx \sqrt{2/(k_f^2 r_p^2 \ln(r_c/r_p))}$ (assuming that $k_f r_c \ll 1$).[35] For typical experiments, $k_\perp \gtrsim 1-10$, and several previous publications[28,29,33] focussed on this regime, although $k_\perp < 1$ is achievable.[32] Here, we make no assumptions about the size of $k_\perp$.

These equations admit an infinite number of integral invariants. The most important of these for our purposes are total particle number $\mathscr{N}$, total momentum $\mathscr{P}$, and total energy $\mathscr{E}$

$$\mathscr{N}=\int_{-\infty}^{\infty} dz N(z,t), \tag{4}$$
$$\mathscr{P}=\int_{-\infty}^{\infty} dz N(z,t)\mathrm{V}(z,t), \tag{5}$$
$$\mathscr{E}=\frac{1}{2}\int_{-\infty}^{\infty} dz N(z,t)\left[\mathrm{V}(z,t)^2+\Phi(z,t)\right]. \tag{6}$$

We describe a finite amplitude pump wave as a steady solution to Eq. (3). Steady traveling wave solutions to Eq. (3) depend on z and t only through the combination $s \equiv z-ut$, where u is the wave phase velocity and s is the position measured in the wave frame. For these steady solutions, Eq. (3) simplify to

$$\frac{\partial}{\partial s}(VN)=0,$$
$$\frac{\partial}{\partial s}\left(\frac{1}{2}V^2+\Phi\right)=0,$$
$$\frac{\partial^2\Phi}{\partial s^2}-k_\perp^2\Phi=-N+1, \tag{7}$$

where $V(s) \equiv \mathrm{V}(s)-u$ is the fluid velocity measured in the wave frame. These coupled ordinary differential equations (ODEs) can be solved in various ways. Here, we briefly review the Fourier method, whereby we impose the 2π periodicity required by our choice of units by writing the solutions as Fourier series

$$N(s)=\sum_{m=-\infty}^{\infty} N_m \exp(ims),$$
$$V(s)=\sum_{m=-\infty}^{\infty} V_m \exp(ims), \tag{8}$$
$$\Phi(s)=\sum_{m=-\infty}^{\infty} \Phi_m \exp(ims).$$

For simplicity, we choose the origin of s so that the solutions are even in s, implying that Fourier coefficients satisfy $N_{-m}=N_m$ and similarly for V_m and Φ_m. Since N, V, and Φ are real functions, this choice implies that the Fourier coefficients are also real.

Applying these Fourier expansions to Eq. (7) yields the following coupled equations for the Fourier coefficients:

$$m\sum_n V_{m-n}N_n=0,$$
$$m\Phi_m+m\sum_n \frac{1}{2}V_{m-n}V_n=0,$$
$$\Phi_m=\frac{N_m-\delta_{m,0}}{m^2+k_\perp^2}. \tag{9}$$

Nontrivial solutions to these equations are then found by imposing the following three conditions. First, the amplitude A of the pump wave is defined by setting

$$N_1=N_{-1}=A. \tag{10}$$

Next, the conservation of particle number $\mathscr{N}$ implies that the perturbed density averaged over a wave period must equal the equilibrium density. Thus, the $m=0$ Fourier coefficient of the density is

$$N_0=1. \tag{11}$$

Finally, we define the lab frame as the frame in which there is no net momentum in the fluid ($\mathscr{P}=0$), so $\int_0^{2\pi} N(s)\mathrm{V}(s)ds=0$. Using Eq. (11) and $V(s)=\mathrm{V}(s)-u$, this implies

$$\sum_m N_m V_{-m}=-u.$$

If we define

$$V_0 \equiv -u' \tag{12}$$

and apply Eq. (11), this can be rewritten as

$$u=u'-\sum_{m\neq 0} N_m V_{-m}. \tag{13}$$

Then, Eq. (9) are solved numerically for a given wave amplitude A. The equations are solved for the unknowns u' and a finite number of Fourier coefficients $N_m, m=2,\ldots,P$, and V_m and Φ_m, $m=1,\ldots,P$ (making $3P$ unknowns) for the given values of $k_\perp$ and A, keeping a sufficient number P of Fourier harmonics to achieve convergence. Note that since the $m=0$ equations are trivial, and $m<0$ gives no extra information, there are then $3P$ independent equations for the $3P$ unknowns.

A few examples of these solutions are shown in Fig. 1. Note that the fluid velocity $V(s)$ is negative (for rightward wave propagation) because we work in the wave frame where the fluid flows through the wave from right to left (in the $-s$ direction). For small A, the pump wave is essentially a single Fourier mode with the linear phase velocity u_k of TG waves with wavenumber $k=1$ (in our scaled units). For general wavenumber k

$$u_k=\frac{1}{\sqrt{k^2+k_\perp^2}}, \tag{14}$$

and so, the pump wave phase velocity is $u_1=1/\sqrt{1+k_\perp^2}$ when $A \ll 1$. (There is a second solution with $u=-u_1$, a wave propagating in the $-z$ direction. Throughout this paper, we assume that the pump wave propagates in the $+z$ direction.) Expansions in small A have

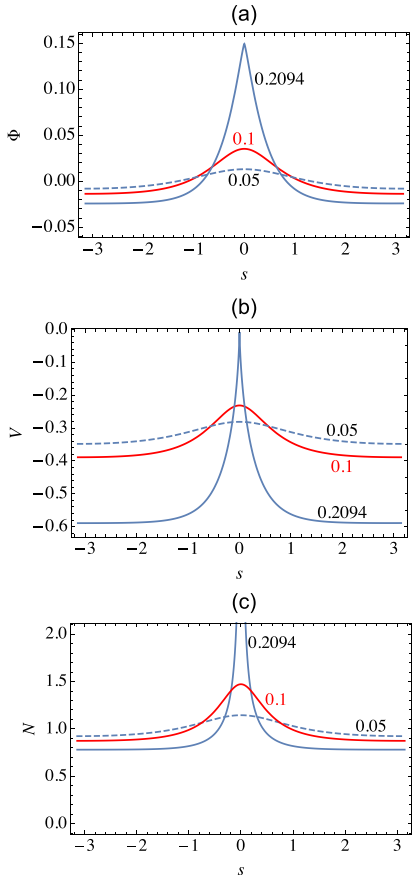

FIG. 1. Plots over one wavelength in position s of (a) the pump wave potential $\Phi(s)$, (b) fluid velocity in the wave frame $V(s)$, and (c) density $N(s)$, taking $k_\perp = 3$, and for 3 different wave amplitudes: $A = 0.05$, 0.1, and $A_{max} = 0.2094$, the maximum amplitude at this $k_\perp$ value.

been carried out,[33] where it has been shown that the finite amplitude corrections to u' and u take the form of a power series in A^2

$$u'/u_1 = 1 + \frac{1}{4}A^2(8 + 3k_\perp^2) + \frac{1}{64}A^4(128 + 208k_\perp^2 + 65k_\perp^4 + 3k_\perp^6) + O(A^6), \quad (15)$$

$$u/u_1 = 1 + \frac{3}{4}A^2k_\perp^2 + \frac{3}{64}A^4k_\perp^2(16 + 11k_\perp^2 + k_\perp^4) + O(A^6). \quad (16)$$

The coefficients in the power series for these first terms are positive, implying an increasing phase speed with increasing pump wave amplitude.

It was also shown that the Fourier coefficients of density and velocity obey the ordering

$$N_m, V_m \approx O(A^{|m|}) \quad (17)$$

for small A, which follows from the simple quadratic nonlinearities in Eq. (7). For example, for a rightward propagating pump wave,

$$V_1 = Au_1 + O(A^3), \quad (18)$$

$$N_2 = \frac{3}{2}A^2\frac{u_1^2}{u_1^2 - u_2^2} + O(A^4), \quad (19)$$

$$V_2 = \frac{u_1}{2}A^2\frac{u_1^2 + 2u_2^2}{u_1^2 - u_2^2} + O(A^4). \quad (20)$$

The pump wave becomes more sharply peaked with increasing amplitude, as its Fourier harmonics with $|m| > 1$ become appreciable. For given $k_\perp$, there is a maximum possible value of A, $A_{max}(k_\perp)$, corresponding to a wave for which the maximum value of $V(s)$ approaches zero from below, a stagnation point in the wave [see Fig. 1(b)]. At this amplitude, the cold fluid theory breaks down: the density is singular at this point, and both the fluid velocity and potential have a slope discontinuity. Kinetic effects such as particle trapping in the wave potential then become important.[30] As $k_\perp$ increases, $A_{max}(k_\perp)$ decreases (Fig. 2). This is because increasing $k_\perp$ makes the linear wave dispersion relation more acoustic (i.e., less dispersive): see Eq. (14), which approaches constant phase speed $u_k = 1/k_\perp$ for large $k_\perp$. These nonlinear wave equilibria exist through a balance between nonlinearity (which would cause the waves to steepen) and dispersive spreading. In order for this balance to be maintained for a less-dispersive (larger $k_\perp$) wave, the wave must be less nonlinear, so the maximum pump amplitude must be smaller.

III. FLUID STABILITY

A. General Considerations

In this section, we consider the stability with respect to small perturbations of a nonlinear pump wave with given amplitude A and fundamental wavenumber $k = 1$ in our scaled units. We will consider stability using fluid theory. We will work in the frame of the pump wave and consider small perturbations to the density, fluid velocity, and potential of the form $N(z,t) = N(s) + \delta N(s,t)$, $V(z,t) = V(s) + u + \delta V(s,t)$, and $\Phi(z,t) = \Phi(s) + \delta\Phi(s,t)$. Linearizing Eq. (3) in the perturbations yields

$$\frac{\partial \delta N}{\partial t} + \frac{\partial}{\partial s}[V(s)\delta N + N(s)\delta V] = 0, \quad (21)$$

$$\frac{\partial \delta V}{\partial t} + \frac{\partial}{\partial s}[V(s)\delta V + \delta\Phi] = 0, \quad (22)$$

$$\frac{\partial^2 \delta\Phi}{\partial s^2} - k_\perp^2\delta\Phi = -\delta N. \quad (23)$$

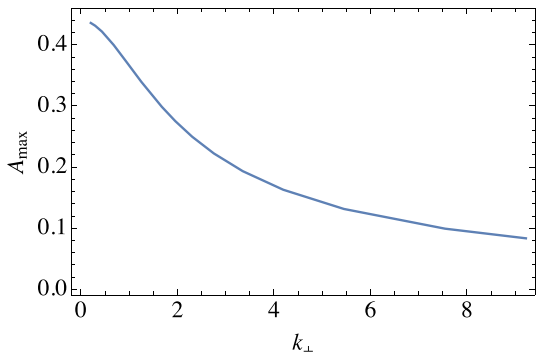

FIG. 2. Maximum amplitude A of the first Fourier coefficient of the density in a TG traveling pump wave vs perpendicular wavenumber $k_\perp$.

We solve these equations assuming periodic boundary conditions for the perturbed quantities, with a period that is some integer multiple M of the pump wavelength. In a previous publication,[33] we considered only $M=2$ (a case of importance in the parametric decay instability), but here we generalize to any $M \geq 1$. In the limit $M \to \infty$, perturbations with any functional form are allowed.

The energy of a perturbation on the pump wave is a conserved quantity (i.e., time-independent), since the total energy (6) is conserved. The consideration of this energy integral is quite useful in stability analysis. Working in the frame of the pump wave, the wave energy is[37]

$$\mathscr{E} - u\mathscr{P} = \frac{1}{2}\int ds N(s,t)\left[V(s,t)^2 + \Phi(s,t)\right] - \frac{1}{2}u^2\mathscr{N}. \tag{24}$$

Using the assumed periodic nature of the system, we consider the perturbed energy E per unit length

$$\begin{aligned} E = {} & \frac{1}{4\pi M}\int_0^{2\pi M} ds\{2N(s)V(s)\delta V(s,t) + \delta N(s,t)V(s)^2 \\ & + \delta N(s,t)\Phi(s) + N(s)\delta\Phi(s,t) - u^2\delta N(s,t)\} \\ & + \frac{1}{4\pi M}\int_0^{2\pi M} ds\{N(s)[\delta V(s,t)]^2 + 2V(s)\delta N(s,t)\delta V(s,t) \\ & + \delta\Phi(s,t)\delta N(s,t)\}. \end{aligned} \tag{25}$$

The terms that are linear in the perturbations can all be dropped thanks to Eqs. (7) and (21)–(23). For example, the first term in E involves $N(s)V(s)$, but Eq. (7) imply that this combination is constant, so the term is proportional to the spatial average of $\delta V(s,t)$. However, this average is time-independent according to the integral over s of Eq. (22). In fact, since we work in the frame of the pump wave, the average value of δV vanishes, so the first term in E is zero. The other linear perturbation terms in E can also be shown to vanish, because the spatial average of δN vanishes due to the conservation of the particle number. This leaves the quadratic terms in E

$$\begin{aligned} E = {} & \frac{1}{4\pi M}\int_0^{2\pi M} ds\{N(s)[\delta V(s,t)]^2 \\ & + 2V(s)\delta N(s,t)\delta V(s,t) + \delta\Phi(s,t)\delta N(s,t)\}. \end{aligned} \tag{26}$$

The first and second terms in the integrand are perturbations to the kinetic energy, and the last term is the perturbed electrostatic potential energy. Using Eq. (23), one can show that the last term is non-negative and so is the first term. However, the second kinetic energy term can be either positive or negative. Thus, perturbations, as seen in the wave frame, can have positive energy, negative energy, or even zero energy.

In fact, it is the zero energy perturbations which are most interesting from the standpoint of instability, for the following simple reason: energy conservation implies that *only zero energy perturbations can be unstable*. Equation (26) shows that E is proportional to the square of the amplitude of a given perturbation. An unstable growing perturbation, with exponentially increasing amplitude, must then have increasing energy magnitude, an impossibility unless the perturbation has zero energy.

Zero-energy excitations are often linked to instability. One familiar situation where they occur in fluids is in the growth of a perturbation on a gravitationally unstable fluid interface (the Rayleigh-Taylor instability[36]) where kinetic energy of a perturbation grows at the expense of reduced potential energy, such that the total energy is conserved. For nonlinear TG waves with non-negative perturbed potential energy, we will find that zero-energy excitations occur instead over fairly narrow wavenumber ranges associated with the occurrence of wave degeneracies. Rather than trading kinetics for potential energy in a single growing wave, the instability trades energy between two resonant waves whose energies are of opposite sign.

We will now examine the stability of the solutions to Eqs. (21)–(23) by considering complex eigenmodes of the equations, for which the time dependence of perturbed quantities is of the form $\exp(-i\omega t)$, where ω is a (possibly complex) eigenfrequency. A more general perturbation can be written as a sum of these eigenmodes, and the real part is then taken to obtain physically relevant results. The complex eigenmode equations can be elegantly written as a single vector equation[30]

$$i\omega\psi(s) = \hat{L}\cdot\psi(s), \tag{27}$$

where the vector eigenmode $\psi(s) \equiv (\delta N(s), \delta V(s))$, $\delta N(s)$ and $\delta V(s)$ are the spatial form of the density and velocity perturbations, respectively, associated with the eigenmode, and the linear matrix operator $\hat{L}(s)$ is defined as

$$\hat{L} = \frac{\partial}{\partial s}\begin{pmatrix} V(s) & N(s) \\ \hat{G} & V(s) \end{pmatrix}. \tag{28}$$

Here, $\hat{G}$ is the Green function operator for the solution to the Poisson equation, Eq. (23), defined as

$$\hat{G}\delta N(s) = \int_0^{2\pi M} d\bar{s} g(s,\bar{s})\delta N(\bar{s}) = \delta\Phi(s), \tag{29}$$

where the Green function $g(s,\bar{s})$ satisfies

$$\frac{\partial^2 g(s,\bar{s})}{\partial s^2} - k_\perp^2 g(s,\bar{s}) = -\delta(s-\bar{s}) \tag{30}$$

solved with periodic boundary conditions of period $2\pi M$.

The matrix operator $\hat{L}$ has some important features that determine the properties of its eigenmodes. First, the operator is real-valued: $\hat{L} = \hat{L}^*$. This implies that, if $\psi(s)$ is a vector eigenfuction of $\hat{L}$, with frequency ω, then $\psi^*(s)$ is also an eigenfunction, with frequency $-\omega^*$. This follows by taking the complex conjugate of Eq. (27). Thus, eigenmodes come in complex-conjugate pairs.

Next, the operator $\hat{L}$ is periodic in s, with period 2π (the pump wavelength in our scaled units). Floquet's theorem[38] can therefore be applied to the eigenmodes arising from the solution of Eq. (27), implying that the general spatial form of an eigenmode is a doubly periodic function: a product of some periodic vector function with period 2π (written below as a Fourier series with vector coefficients χ_m) and $\exp(iks)$

$$\psi(s) = \exp(iks)\sum_{m=-\infty}^{\infty}\chi_m \exp(ims), \tag{31}$$

for any value of the wavenumber k that matches the boundary conditions: $k = n/M$ for integer n. (Floquet's theorem also allows the possibility of exponentially growing and decaying solutions in s, but these are disallowed by the periodic boundary conditions.) Physically, this

form of the eigenmode arises because a Fourier component of the eigenmode with the wavenumber k mode couples to component $k+m$, for integer m, through the mth Fourier component of the pump wave.

Finally, the operator $\hat{L}$ can be shown to be anti-Hermitian (also often referred to as skew-Hermitian) with respect to vector functions ψ that satisfy the periodic boundary conditions of period $2\pi M$ and with respect to a generalized matrix inner product defined by its action on any two such functions $\psi_1 = (\delta N_1, \delta V_1)$ and $\psi_2 = (\delta N_2, \delta V_2)$

$$[\psi_1, \psi_2] \equiv \frac{1}{8\pi M}\int_0^{2\pi M} ds\, \psi_1^*(s) \cdot \begin{pmatrix} \hat{G}^\dagger & V(s) \\ V(s) & N(s) \end{pmatrix} \cdot \psi_2(s), \tag{32}$$

where $\hat{G}^\dagger$ is the left Green function operator, which defined as

$$\delta N \hat{G}^\dagger(s) = \int_0^{2\pi M} d\bar{s} g(s,\bar{s}) \delta N(\bar{s}) = \delta\Phi(s), \tag{33}$$

with $g(s,\bar{s})$ the same Green function as in Eq. (30). This inner product differs by a normalization factor compared to that used in Ref. 30, for notational convenience.

The anti-Hermitian property of $\hat{L}$, defined by the expression

$$[\psi_1, \hat{L}\cdot\psi_2] = -[\psi_2, \hat{L}\cdot\psi_1]^*, \tag{34}$$

can be proven by using integration by parts, with boundary terms canceling due to the periodic boundary conditions.

It is also useful to note that this anti-Hermitian property of $\hat{L}$ is equivalent to the statement that the operator $-i\hat{L}$ is pseudo-Hermitian[39] with respect to the above generalized matrix inner product.

This anti-Hermitian (or pseudo-Hermitian) property has several well-known implications for the eigenmodes of the operator. Let us assume that ψ_1 and ψ_2 in Eq. (34) are any two vector eigenfunctions with frequencies ω_1 and ω_2, respectively. Then, Eqs. (34) and (27) yield

$$i\omega_2[\psi_1, \psi_2] = i\omega_1^*[\psi_2, \psi_1]^*. \tag{35}$$

However, inner products have the property that $[\psi_2, \psi_1]^* = [\psi_1, \psi_2]$. [For our inner product, this identity relies on the symmetry property

$$\int_0^{2\pi M} ds \delta\Phi_1^*(s)\delta N_2(s) = \int_0^{2\pi M} ds \delta\Phi_2(s)\delta N_1^*(s), \tag{36}$$

which can be proven through integration by parts, using Eq. (23).] Applying this identity to Eq. (35) implies that

$$i(\omega_2 - \omega_1^*)[\psi_1, \psi_2] = 0. \tag{37}$$

Thus, if $\omega_2 \neq \omega_1^*$, ψ_1, and ψ_2 are orthogonal with respect to the inner product. For example, if we take $\psi_2 = \psi_1^*$ so that $\omega_2 = -\omega_1^*$, Eq. (37) implies $\omega_1^*[\psi_1, \psi_1^*] = 0$. Thus, ψ_1 is orthogonal to its complex conjugate eigenmode ψ_1^* for all eigenmodes, except possibly for any that happen to have zero frequency.

Now, consider another case where we take $\psi_1 = \psi_2$ in Eq. (37) (and so $\omega_1 = \omega_2$). Then, the equation reduces to

$$(\omega_1 - \omega_1^*)[\psi_1, \psi_1] = 0. \tag{38}$$

Thus, $\omega_1 = \omega_1^*$, or in other words ω_1 is real, *provided that* $[\psi_1, \psi_1] \neq 0$. This important caveat was left out of the discussion in Ref. 30. Therefore, all eigenmodes ψ_1 for which $[\psi_1, \psi_1] \neq 0$ are stable.

However, while standard inner products have the property that $[f,f] > 0$ for any nontrivial function f, our generalized inner product does not have this property. Equation (32) implies that

$$\begin{aligned}[\psi_1, \psi_1] = \frac{1}{8\pi M}\int_0^{2\pi M} ds \{ & N(s)|\delta V_1(s)|^2 \\ & + V(s)\left[\delta N_1(s)^*\delta V_1(s) + \delta V_1(s)^*\delta N_1(s)\right] \\ & + \delta\Phi_1(s)\delta N_1(s)^*\}.\end{aligned} \tag{39}$$

Although this inner product must be real [the potential energy term is real because of Eq. (36)], its sign is indeterminate: it can be negative, positive, or zero. The sign of such generalized inner products is often referred to as the "Krein sign."[40] In fact, compared to Eq. (26), one can see that

$$[\psi_1, \psi_1] = E_1, \tag{40}$$

where E_1 is the energy change associated with the eigenmode perturbation $\mathrm{Re}\,\psi_1 \exp(-i\omega_1 t)$. As discussed previously, this energy change can be positive, negative, or zero. Equations (38) and (40) show again that only $E_1 = 0$ allows the possibility of growing (or decaying) modes. All the other eigenmodes, with nonzero energy, are stable.

B. Small Amplitudes and the Conditions for Instability

While zero energy eigenmodes allow the possibility of instability, not all such eigenmodes are unstable. One zero energy eigenmode is a simple shift of the pump wave in position by the infinitesimal amount ds: $\psi = ds(\partial N/\partial s, \partial V/\partial s)$. This eigenmode clearly has zero frequency as well as zero energy and so is not unstable.

Under the right circumstances, other zero-energy eigenmodes can occur. To see how this happens, consider the case of a small amplitude pump, $A \ll 1$, and take $M \to \infty$. Then, to zeroth order in A, the eigenmodes are linear waves with s dependence $\exp(iks)$ for some wavenumber $k \in \mathrm{Re}$, propagating in a uniform density plasma that moves in the $-z$ direction with speed $u = u_1 = 1/\sqrt{1+k_\perp^2}$ as seen in the frame of the infinitesimal pump wave [see Eq. (14)]. The zeroth-order eigenmode frequency for given wavenumber k is found by Fourier transforming Eq. (27), yielding

$$\omega = \omega_k^\pm \equiv -ku_1 \pm ku_k, \tag{41}$$

where u_k is the linear phase speed as seen in the lab frame, given by Eq. (14).

For a given wavenumber k, there are two eigenmodes ψ_k^+ and ψ_k^-, with frequencies $\omega_k^\pm$ corresponding to the two signs in Eq. (41). These are waves propagating to the right or to the left when viewed in the lab frame, having the lowest-order form

$$\psi_k^\pm(s) = \exp(iks)\begin{pmatrix} 1 \\ \pm u_k \end{pmatrix}. \tag{42}$$

The energies $E_k^\pm$ associated with these zeroth-order eigenmodes follow from Eqs. (42), (39), and (40) and the Fourier transform of Eq. (23),

$$E_k^{\pm} = \frac{1}{2}\left(u_k^2 \mp u_1 u_k\right). \tag{43}$$

The energy E_k^- is positive for any k, but E_k^+ can be positive or negative $E_k^+ > (<)0$ if $u_k > (<)u_1$.

For $k = \pm 1$, the + mode has zero energy, so one might expect an instability here. However, the component of either the $k = 1$ or the $k = -1$ + mode that is 90° out of phase with the pump is simply the translation of the pump wave discussed previously; it is not unstable. The in-phase component produces a change in the amplitude of the pump wave, but this is also not an instability. The energy shift due to amplitude change is not really zero, and it is just higher order in A than Eq. (43).

Now, we are in a position to understand how instability can develop in this system. As discussed in relation to Eq. (31), the pump wave causes mode-coupling between these zeroth-order eigenmodes. For small but finite A, the mode coupling changes the form of a given eigenmode ψ_k^α (where $\alpha = +$ or $-$ labels the branches of the dispersion relation), but the eigenmode (usually) remains close to ψ_k^α. Then, we can write Eq. (31) in the form

$$\psi(s) = \psi_k^\alpha + c_0^{\alpha^\dagger}\psi_k^{\alpha^\dagger} + \sum_{m\neq 0}(c_m^+\psi_{k+m}^+ + c_m^-\psi_{k+m}^-), \tag{44}$$

where $\alpha^\dagger$ is the opposite branch of the dispersion relation to α; i.e., if $\alpha = +$, then $\alpha^\dagger = -$ and vice versa. The coefficient $c_0^{\alpha^\dagger}$ multiplying the second term arises from the reflection of the wave off of the pump and into the other branch of the dispersion relation (reversing its phase velocity as seen in the lab frame) and is small, typically of order A^2. The other coefficients c_m^α arise from mode-coupling with the mth Fourier harmonic of the pump wave and are also typically small, of order $A^{|m|}$, because of Eq. (17). The mode frequency is also shifted from ω_k^α by a small amount, typically by order A^2, and the energy is also shifted by a small amount, leaving it nonzero (except for the case $k \simeq \pm 1$ for which $E_k^+ \simeq 0$, which will be considered below in the discussion of modulational instability). Since the eigenmode energy is nonzero, the system remains stable. These scalings can be obtained by applying nondegenerate perturbation theory to Eq. (27).

However, an exception to these scalings occurs when a degeneracy occurs between the zeroth-order mode frequency ω_k^α and one of the other coupled modes in Eq. (44) with frequency ω_{k+m}^β. These two degenerate modes are the "daughter waves" mentioned previously. For any particular wavenumber k where

$$\omega_k^\alpha = \omega_{k+m}^\beta, \tag{45}$$

there is a resonant interaction between ψ_k^α and ψ_{k+m}^β, moderated by the pump wave, which allows energy to be traded between these two components of the eigenmode. Then, c_m^β is no-longer small. The eigenmode is now given by

$$\psi(s) = C_1\psi_k^\alpha + C_2\psi_{k+m}^\beta + \Delta\psi, \tag{46}$$

with $\Delta\psi$ small (of order A) and C_1 and C_2 of order unity.

The degeneracy is not in itself enough to cause instability in the system. However, if daughter wave ψ_k^α has energy E_k^α that is *opposite in sign* to that of the other wave, E_{k+m}^β, instability occurs. The positive energy daughter wave gains energy resonantly from the negative energy wave, allowing it to grow in amplitude. Loss of energy from the negative energy wave *increases* the amplitude of this wave as well, and the amplitude of both daughter waves can then continue to grow exponentially, in a feedback loop.

To show mathematically that an instability arises from degenerate daughter waves with energies of opposite signs, we use the fact that an unstable perturbation must have zero energy [see Eqs. (38) and (40)]. When Eq. (46) is used in Eqs. (26), (38), and (40), and only zeroth-order terms in A are kept, we obtain the following energy relation for the unstable daughter waves:

$$E = E_k^\alpha|C_1|^2 + E_{k+m}^\beta|C_2|^2 = 0. \tag{47}$$

For nonzero daughter wave amplitudes and energies, this equation can only be satisfied when their energies are opposite in sign. This proves that growth (or decay) only occurs if the resonant daughter waves have energies of opposite sign, as seen in the pump wave frame.

These energy arguments are general, relying only on the quadratic form of the energy integral at small amplitude. They apply to the instability of a pump wave in any ideal fluid system.

Let us now consider the degeneracy condition, Eq. (45), for TG modes, using the linear dispersion relation Eq. (41) for the daughter wave frequencies. There are three separate cases: $\omega_k^+ = \omega_{k+m}^+$, $\omega_k^- = \omega_{k+m}^+$, and $\omega_k^- = \omega_{k+m}^-$, shown in Figs. 3–5. Figure 4 shows that $\omega_k^- = \omega_{k+m}^-$ has no solutions and need not be considered further. Also, for the other two cases, degeneracies occur at $k = \pm 1$ and $k = 0$. Waves with $k = 0$ correspond to changes in the background plasma parameters and do not by themselves lead to instability. On the other hand, the degeneracies at $k = \pm 1$ contribute to the modulational instability, considered later.

The only case to give degeneracies at $k \neq 0$ or ± 1 is the case $\omega_k^- = \omega_{k+m}^+$. Figure 5 shows that for given m, a single degeneracy occurs at a value of k depending on $k_\perp$ that we refer to as $k_0(k_\perp)$, provided that m is not too much larger than $k_\perp$. For sufficiently large m, there are no solutions. Figure 6 shows how $k_0(k_\perp)$ behaves for a few different values of m. In the large $k_\perp$ limit, an asymptotic expansion of the dispersion relations yields

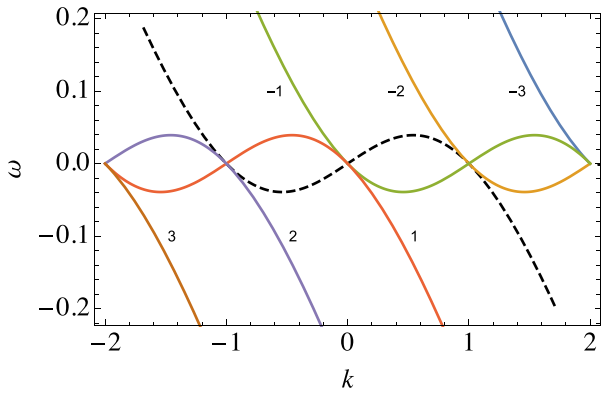

FIG. 3. A plot of ω_k^+ (dashed) and ω_{k+m}^+ vs wavenumber k, for several values of m, with the curves labeled by m, and for $k_\perp = 3/2$. Degeneracies occur where the dashed curve crosses one of the other curves. The only degeneracies occur at $k = 0$ and $k = \pm 1$. The $k = \pm 1$ degeneracies result in modulational instability.

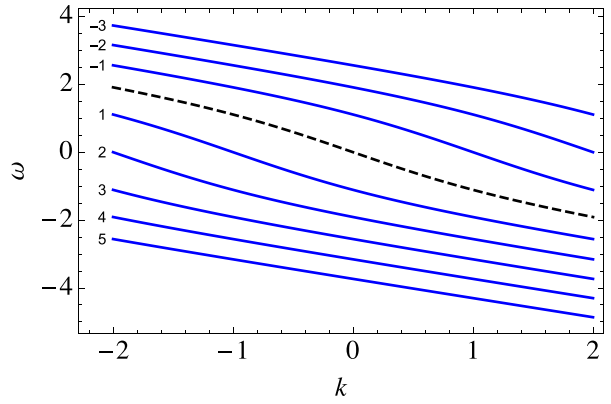

FIG. 4. A plot of ω_k^- (dashed) and ω_{k+m}^- for several values of m, with the curves labeled by m, and for $k_\perp = 3/2$. There are no degeneracies.

$$\lim_{k_\perp \to \infty} k_0(k_\perp) = \frac{m(m^2-1)}{4k_\perp^2}, \tag{48}$$

and for small $k_\perp$, the only degeneracy of this type occurs for $|m| = 2$, at $|k_0| = \sqrt{3} - 1$ as $k_\perp \to 0$.

We will find that there are very narrow regions of k around these degeneracies over which the pump wave is unstable. Note that if M is not too large, it is somewhat unlikely that any of these unstable regions intersect with the quantized k values $k = n/M$. Intersections will occur only for small ranges of $k_\perp$ (that also depend on amplitude A, since the degeneracies are shifted by nonlinearity). Thus, in Ref. 33 where only $M = 2$ was considered, no traveling wave instabilities were found for the $k_\perp$ values tested.

Expressions for the growth rate can be obtained using degenerate perturbation theory. We first examine the case for which $m = 1$ or -1 in Eq. (45), which can be handled with first-order degenerate perturbation theory. This is the case which leads to three-wave instability and the parametric decay instability, a type of 3-wave instability where the wavenumbers k and $k \pm 1$ have magnitudes that add to 1 (for instance,

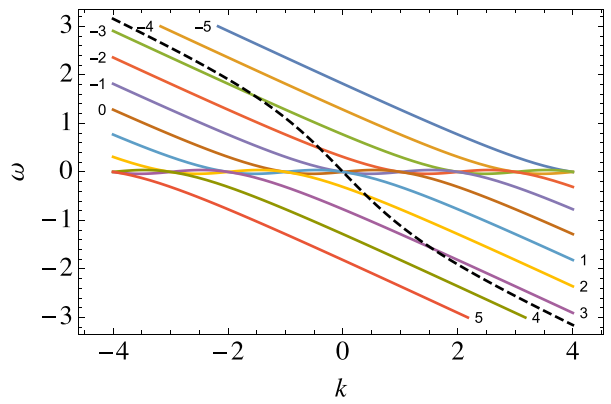

FIG. 5. A plot of ω_k^- (dashed) and ω_{k+m}^+ for several values of m, with the curves labeled by m, and for $k_\perp = 3/2$. Degeneracies occur where the dashed curve crosses one of the other curves. Four $k \neq 0$ degeneracies occur, for $m = -3, -2, 2$, and 3.

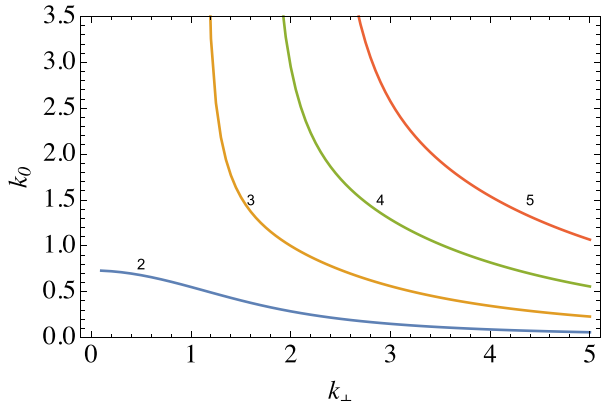

FIG. 6. The nontrivial degeneracies found from the solution of $\omega_k^- = \omega_{k+m}^+$, plotted vs $k_\perp$ for 4 values of m.

$k = -1/2$ and $k + 1 = 1/2$), so that the pump wave decays into two daughter waves of longer wavelength. However, for TG waves, Eqs. (41) and (14) imply that $\omega_k^\alpha = \omega_{k\pm1}^\beta$ "only" at $k = 0$, 1, or -1 (depending on α, β, and the $\pm$ sign; see Figs. 3 and 5), and the mode coupling at these degeneracies is such that the TG system is not 3-wave unstable.

Nevertheless, this $m = \pm 1$ case is the easiest case to analyze and applies to many systems other than TG modes, so we will analyze it first, leaving the form of the dispersion relation general, allowing the possibility of 3 wave resonances to occur for values of k other than 0, 1, or -1. We take the case $m = 1$ (the $m = -1$ case can be obtained from the $m = 1$ case by interchanging indices and redefining k) and assume that there is a degeneracy that occurs for wavenumber $k = k_0$, at which point

$$\omega_{k_0}^\alpha = \omega_{k_0+1}^\beta \equiv \omega_0. \tag{49}$$

To analyze the stability near this degeneracy in first-order perturbation theory, we break $\hat{L}$ into an equilibrium portion $\hat{L}_0$ and a portion of order A due to the pump wave: $\hat{L} = \hat{L}_0 + \Delta\hat{L}$, where

$$\hat{L}_0 = \frac{\partial}{\partial s}\begin{pmatrix} -u_1 & 1 \\ \hat{G} & -u_1 \end{pmatrix} \tag{50}$$

and

$$\Delta\hat{L} = 2A\frac{\partial}{\partial s}\cos s\begin{pmatrix} u_1 & 1 \\ 0 & u_1 \end{pmatrix} + O(A^2). \tag{51}$$

These expressions follow from the Fourier expansions of the pump wave given in Eqs. (8), (10)–(12), (15), and (18). We then substitute Eq. (46) into Eq. (27), noting that the zeroth-order eigenmodes ψ_k^α satisfy the zeroth order eigenvalue problem $i\omega_k^\alpha\psi_k^\alpha = \hat{L}_0\psi_k^\alpha$

$$\begin{aligned} i\omega(C_1\psi_k^\alpha + C_2\psi_{k+1}^\beta + \Delta\psi) = {} & iC_1\omega_k^\alpha\psi_k^\alpha + iC_2\omega_{k+1}^\beta\psi_{k+1}^\beta \\ & + \Delta\hat{L}(C_1\psi_k^\alpha + C_2\psi_{k+1}^\beta) + (\hat{L}_0 + \Delta\hat{L})\Delta\psi. \end{aligned} \tag{52}$$

We drop the $\Delta\hat{L}\Delta\psi$ term since we work only to first order in A. Noting that the zeroth order eigenmodes are orthogonal with respect to the zeroth order inner product

$$[\psi_1,\psi_2]_0 \equiv \frac{1}{8\pi M}\int_0^{2\pi M} ds\,\psi_1^*(s)\cdot\begin{pmatrix}\hat{G}^\dagger & -u_1\\ -u_1 & 1\end{pmatrix}\cdot\psi_2(s) \tag{53}$$

and that the operator $\hat{L}_0$ is anti-Hermitian with respect to this inner product, we take an inner product of Eq. (52) with ψ_k^α, which removes terms involving $\Delta\psi$ (since $\Delta\psi$ is orthogonal to the two daughter waves, by construction). The result is

$$i\omega C_1\left[\psi_k^\alpha,\psi_k^\alpha\right]_0 = i\omega_k^\alpha C_1\left[\psi_k^\alpha,\psi_k^\alpha\right]_0 + C_1\left[\psi_k^\alpha,\Delta\hat{L}\psi_k^\alpha\right]_0 + C_2\left[\psi_k^\alpha,\Delta\hat{L}\psi_{k+1}^\beta\right]_0. \tag{54}$$

The inner products can then be evaluated using Eqs. (53), (51), and (42). We obtain $[\psi_k^\alpha,\psi_k^\alpha]_0 = E_k^\alpha$. Also, we only need to work to first-order in A to obtain nontrivial results, and we find that $[\psi_k^\alpha,\Delta\hat{L}\psi_k^\alpha]_0 = O(A^2)$, so this term can be dropped. The other $\Delta\hat{L}$ term yields

$$\left[\psi_k^\alpha,\Delta\hat{L}\psi_{k+1}^\beta\right]_0 = iA\frac{\omega_k^\alpha}{4}\left\{u_1(\alpha u_k+\beta u_{k+1})+\alpha\beta u_k u_{k+1}\right\} \equiv iAL_{k,k+1}^{\alpha,\beta}, \tag{55}$$

where we employ the notational convenience that multiplication by $\alpha = +$ or $-$ means multiplication by $+1$ or -1, respectively, and similarly for β. Then, applying an inner product to Eq. (52) with respect to ψ_{k+1}^β, the same procedure yields a second equation, which when combined with Eq. (54) results in the following matrix equation for C_1 and C_2:

$$\begin{pmatrix}E_k^\alpha(\omega-\omega_k^\alpha) & -AL_{k,k+1}^{\alpha,\beta}\\ -AL_{k+1,k}^{\beta,\alpha} & E_{k+1}^\beta\left(\omega-\omega_{k+1}^\beta\right)\end{pmatrix}\cdot\begin{pmatrix}C_1\\ C_2\end{pmatrix} = 0. \tag{56}$$

The off-diagonal matrix coefficients are produced by mode coupling between the two daughter waves in the eigenmode, induced by the pump wave. The coefficient $L_{k+1,k}^{\beta,\alpha}$ can be obtained by interchanging indices in Eq. (55). In this equation, the expression inside the braces is symmetric under this interchange, and this implies that on resonance, where $k = k_0$ and Eq. (49) is satisfied, the two off-diagonal matrix components are identical, so the matrix in Eq. (56) is Hermitian. On resonance, setting the matrix determinant to zero gives

$$E_{k_0}^\alpha E_{k_0+1}^\beta(\omega-\omega_0)^2 - \left(AL_{k0+1,k0}^{\beta,\alpha}\right)^2 = 0, \tag{57}$$

yielding

$$\omega = \omega_0 \pm |A|\frac{\left|L_{k0+1,k0}^{\beta,\alpha}\right|}{\sqrt{E_{k_0}^\alpha E_{k_0+1}^\beta}}. \tag{58}$$

We can see here that growth (or decay) occurs only when the energies of the daughter waves have opposite signs so that the square root yields an imaginary number. Note also that the ratio of $|C_1|^2$ to $|C_2|^2$ implied by Eqs. (58) and (56) agrees with Eq. (47), so the total energy of the eigenmode is indeed zero.

There is a small range of k values around $k = k_0$ which allows growth or decay. Writing $k = k_0 + \Delta k$ and $\omega = \omega_0 + \Delta\omega$ where both Δk and $\Delta\omega$ are of order A, a Taylor expansion of Eq. (56) in Δk gives

$$\begin{pmatrix}E_{k_0}^\alpha(\Delta\omega - v_{k_0}^\alpha\Delta k) & AL_{k_0+1,k_0}^{\beta,\alpha}\\ AL_{k_0+1,k_0}^{\beta,\alpha} & E_{k_0+1}^\beta(\Delta\omega - v_{k_0+1}^\beta\Delta k)\end{pmatrix}\cdot\begin{pmatrix}C_1\\ C_2\end{pmatrix} = 0, \tag{59}$$

where

$$v_k^\alpha = \partial\omega_k^\alpha/\partial k \tag{60}$$

is the daughter wave group velocity. The matrix determinant now yields

$$\Delta\omega = \frac{v_{k_0}^\alpha + v_{k_0+1}^\beta}{2}\Delta k \pm \frac{1}{2}\sqrt{\left(v_{k_0}^\alpha - v_{k_0+1}^\beta\right)^2\Delta k^2 + 4A^2\frac{\left(L_{k0+1,k0}^{\beta,\alpha}\right)^2}{E_{k_0}^\alpha E_{k_0+1}^\beta}}, \tag{61}$$

so the eigenmode is stabilized when Δk is sufficiently large, of order A or larger.

Finally, we note that for the TG wave system, the three-wave resonance condition (49) can occur only for $\omega_0 = 0$, with wavenumber $k_0 = 0$ and $\beta = +$, $\alpha = +$ or $-$ or $k_0 = -1$, $\alpha = +$ and $\beta = +$ or $-$ (see Figs. 3 and 5). However, in each case, one can check that Eq. (59) gives no growth or decay because $E_{\pm1}^+ = 0$ and the off-diagonal elements also vanish (i.e., no mode coupling of zero-frequency modes), but $E_0^\alpha \neq 0$. Thus, 3-wave instability does not occur in the TG wave system.

This result is consistent with the numerical investigations for $M = 2$ performed in Ref. 33, where no parametric instability was observed in the TG system. This paper focussed on the large $k_\perp$ regime for which the wave dispersion is nearly acoustic and considered the apparent near-degeneracy between waves with $k = -1/2$, $\alpha = +$ and $k = 1/2$, $\beta = +$. The frequencies of these waves are of equal magnitude and opposite sign, given by $\omega_{1/2}^+ = -\omega_{-1/2}^+ = (u_{1/2} - u_1)/2 \equiv \Delta\Omega/2$, where $\Delta\Omega$ is the difference between the two daughter wave frequencies, referred to as the "frequency detuning" in Refs. 33 and 29. The detuning is small for a near-acoustic dispersion relation for which waves have nearly the same phase speed, and consequently, there is an apparent near-degeneracy between the daughter waves. One might therefore attempt to apply Eq. (56) taking $k_0 = -1/2$ and $\alpha = \beta = +$. In this case, the daughter wave energies are not of opposite sign; in fact, they are equal: $E_{-1/2}^+ = E_{1/2}^+ = u_{1/2}\Delta\Omega/2$. However, now, the "off-diagonal" terms in Eq. (56) are of opposite sign: $L_{k,k+1}^{+,+} = -L_{k+1,k}^{+,+} = Au_{1/2}\Delta\Omega(u_1 + u_{1/2}/2)/4 \approx (3/8)Au_{1/2}u_1\Delta\Omega$. Applying these results to Eq. (56) and taking the determinant yield

$$\omega = \frac{1}{2}\sqrt{\Delta\Omega^2 - \frac{9}{4}A^2u_1^2}, \tag{62}$$

which exhibits instability for sufficiently small detuning or sufficiently large wave amplitude. However, as pointed out in Ref. 33, for a nearly acoustic dispersion relation, many waves are nearly degenerate and can also couple to the two daughter waves. If A is sufficiently large in Eq. (62) to overcome detuning and produce an apparent instability, then other near-degenerate harmonics of the two daughter waves cannot be neglected, i.e., $\Delta\psi$ cannot be neglected in Eq. (46) and first-order degenerate perturbation theory is not valid. When the harmonics are kept (via a numerical evaluation of the eigenmodes), the above $k = \pm1/2$ daughter waves are not unstable for $m = \pm1$.

However, higher-order ($|m| > 1$) instabilities *can* occur for a TG pump wave, caused by the true degeneracies apparent in Figs. 3 and 5. These instabilities were not considered in Ref. 33, where the focus was on parametric instability. For $|m| > 1$, the general resonance condition Eq. (45) results in instability with a growth rate scaling like $A^{|m|}$, provided that the resonant daughter waves have energies of opposite sign. The mode coupling equations involve higher-order degenerate perturbation theory, and the details quickly become rather complex, but we will see that the resulting equations can be reduced to a two-by-two matrix equation whose form is analogous to Eq. (56)

$$\begin{pmatrix} E^{\alpha}_{k}(\omega-\omega^{\alpha}_{k})-A^{2}\mathscr{L}^{\alpha}_{k} & -A^{|m|}\mathscr{L}^{\alpha,\beta}_{k,k+m} \\ -A^{|m|}\mathscr{L}^{\beta,\alpha}_{k+m,k} & E^{\beta}_{k+m}\left(\omega-\omega^{\beta}_{k+m}\right)-A^{2}\mathscr{L}^{\beta}_{k+m} \end{pmatrix}\cdot\begin{pmatrix} C_1 \\ C_2 \end{pmatrix}=0, \tag{63}$$

where $\mathscr{L}^{\alpha}_{k}$ and $\mathscr{L}^{\alpha,\beta}_{k,\bar{k}}$ are real-valued mode-coupling coefficients, with their order in A given explicitly in the matrix. Expressions for these coefficients are derived in Appendix A. As in the three-wave analysis, the off-diagonal coefficients become equal for k on-resonance. The diagonal mode-coupling coefficients $\mathscr{L}^{\alpha}_{k}$, $\mathscr{L}^{\beta}_{k+m}$ induce nonlinear frequency shifts that change the location of degeneracy by order A^2 to the shifted resonance location $k=\bar{k}_0$, where

$$\omega^{\alpha}_{\bar{k}_0}+A^{2}\mathscr{L}^{\alpha}_{\bar{k}_0}/E^{\alpha}_{\bar{k}_0}=\omega^{\beta}_{\bar{k}_0+m}+A^{2}\mathscr{L}^{\beta}_{\bar{k}_0+m}/E^{\beta}_{\bar{k}_0+m}\equiv\bar{\omega}_0. \tag{64}$$

This equation can be solved for $\bar{k}_0$ to the lowest order in A, yielding

$$\bar{k}_0-k_0=A^{2}\frac{\mathscr{L}^{\beta}_{k_0+m}E^{\alpha}_{k_0}-\mathscr{L}^{\alpha}_{k_0}E^{\beta}_{k_0+m}}{E^{\alpha}_{k_0}E^{\beta}_{k_0+m}\left(v^{\alpha}_{k_0}-v^{\beta}_{k_0+m}\right)}. \tag{65}$$

On resonance, at $k=\bar{k}_0$, the mode frequency is

$$\omega=\bar{\omega}_0\pm|A|^{|m|}\frac{\left|\mathscr{L}^{\alpha,\beta}_{\bar{k}_0,\bar{k}_0+m}\right|}{\sqrt{E^{\alpha}_{\bar{k}_0}E^{\beta}_{\bar{k}_0+m}}}, \tag{66}$$

which implies a maximum growth rate Γ_{max} of

$$\Gamma_{max}=|A|^{|m|}\frac{\left|\mathscr{L}^{\alpha,\beta}_{\bar{k}_0,\bar{k}_0+m}\right|}{\sqrt{-E^{\alpha}_{\bar{k}_0}E^{\beta}_{\bar{k}_0+m}}}, \tag{67}$$

provided as always that the daughter wave energies are of opposite sign so that $E^{\alpha}_{\bar{k}_0}E^{\beta}_{\bar{k}_0+m}<0$. Growth can occur for a range of k values around $k=\bar{k}_0$. Taking $k=\bar{k}_0+\Delta k$, and expanding the reduced matrix in small Δk, we obtain

$$\omega-\bar{\omega}_0=\frac{v^{\alpha}_{\bar{k}_0}+v^{\beta}_{\bar{k}_0+m}}{2}\Delta k \pm\frac{1}{2}\sqrt{\left(v^{\alpha}_{\bar{k}_0}-v^{\beta}_{\bar{k}_0+m}\right)^{2}\Delta k^{2}+4\frac{\left(A^{|m|}\mathscr{L}^{\alpha,\beta}_{\bar{k}_0,\bar{k}_0+m}\right)^{2}}{E^{\alpha}_{\bar{k}_0}E^{\beta}_{\bar{k}_0+m}}}. \tag{68}$$

This shows that instability occurs for a range of wavenumbers given by

$$|\Delta k|<\frac{2\Gamma_{max}}{|v^{\alpha}_{\bar{k}_0}-v^{\beta}_{\bar{k}_0+m}|}. \tag{69}$$

Equations (66)–(68) describe the growth rate expected at the degeneracies for TG waves shown in Figs. 5 and 6, between the + and − branches of the dispersion relation. Since E^{-}_{k} is greater than zero for all $k\neq 0$, and since Eq. (43) predicts that $E^{+}_{k+m}<0$ at each degeneracy, the daughter wave energies are opposite in sign and the pump wave can be unstable provided that Δk is small enough.

C. Modulational instability

There is one special case which must be separately considered: The case of modulational instability. Modulational instability occurs for an $m=2$ degeneracy (a 4 wave interaction) for which $\alpha=\beta=+$. To zeroth order in A, the eigenmode consists of two near-degenerate daughter waves traveling in the same direction as the pump (as seen in the lab frame), with wavenumbers $k=-1+\Delta k$ and $k+m=1+\Delta k$ and with Δk of order A. According to Eq. (14), one wave has phase speed greater than u_1 and the other has phase speed less than u_1, so Eq. (43) implies that the daughter wave energies are opposite in sign. However, as $\Delta k\to 0$, the daughter wave energies and frequencies vanish and consequently so do the mode coupling coefficients. Growth occurs only for $|\Delta k|>0$, and Eq. (66) does not apply.

However, Eq. (63) can still be used to analyze the instability. As described in Appendix A, this reduced matrix equation must be Taylor-expanded about $\Delta k=0$ and takes the form

$$\begin{pmatrix} \epsilon\Delta\omega+a-b\kappa^{2} & a \\ a & -\epsilon\Delta\omega+a-b\kappa^{2} \end{pmatrix}\cdot\begin{pmatrix} C_1 \\ C_2 \end{pmatrix}=0, \tag{70}$$

where $\kappa\equiv\Delta k/A$ is scaled wavenumber, $A^2\Delta\omega=\omega-Av_1^{+}\kappa$ is the second order eigenmode frequency shift,

$$\epsilon=\frac{1}{2\left(1+k_{\perp}^{2}\right)^{2}}, \tag{71}$$

$$a=\frac{k_{\perp}^{2}}{8\left(1+k_{\perp}^{2}\right)^{5/2}}\frac{1-3k_{\perp}^{2}-9k_{\perp}^{4}}{1+3k_{\perp}^{2}+3k_{\perp}^{4}}, \tag{72}$$

and

$$b=\frac{3k_{\perp}^{2}}{4\left(1+k_{\perp}^{2}\right)^{9/2}}. \tag{73}$$

The term a arises from nonlinear mode coupling, while ϵ is related to mode energy and b is related to linear wave dispersion. The diagonal and off-diagonal mode coupling coefficients in Eq. (70) are identically given by a because, while there is mode coupling giving off-diagonal terms in the matrix, and a nonlinear frequency shift giving diagonal terms, these two effects must be in balance so that $\Delta\omega=0$ as $\kappa\to 0$. As we discussed previously, when the daughter waves have the same wavelength as the pump, they are not unstable: they merely translate the pump and/or change its amplitude slightly, depending on their phase.

The second-order wavenumber-dependent frequency shift arising from Eq. (70) is

$$\Delta\omega = \pm\kappa\frac{\sqrt{b^2\kappa^2 - 2ab}}{\epsilon}. \tag{74}$$

This implies that modulational instability occurs for wavenumbers in the range $0 < \kappa^2 < 2a/b$, provided that $ab > 0$. However, Eqs. (72) and (73) imply that $ab > 0$ only for $0 < k_\perp < \sqrt{(\sqrt{5}-1)/6} = 0.45389\ldots$, because the mode coupling coefficient a passes through zero at this value of $k_\perp$. This range of $k_\perp$ has not been examined in our current experiments on nonlinear TG modes, which have focussed on the more easily accessible range $k_\perp > 1$.

When $ab > 0$, the maximum growth rate occurs for daughter waves with the wavenumber given by $|\kappa| = \sqrt{a/b}$, implying a growth rate $\Gamma_{\max} = A^2 a/\epsilon$ (where we have added in the scaling with pump wave amplitude A). This maximum growth rate is plotted vs $k_\perp$ in Fig. 7, over the range of $k_\perp$ where growth occurs. Given that there is a maximum possible pump wave amplitude A that is less than roughly 0.4 (see Fig. 2), the growth rate in this instability for TG waves is rather small.

The special features arising from the symmetry of the modulational instability for TG waves are quite similar to the features seen in the modulational instability of Stokes waves.[1,2,8,10] In Stokes waves, there is also a change from instability to stability as a system parameter is varied (in the case of the Stokes waves, the ratio of the fluid depth to the pump wavelength).

D. Numerical evaluation of eigenmodes

Equation (27) can be solved numerically for the frequency and eigenfunction of eigenmodes in a variety of ways. We have done so here using a Fourier method (a variant of Hill's method[27]) based on Eq. (31). We decompose a given eigenmode in terms of the zeroth order modes ψ_k^α, which is equivalent to the Fourier expansion used in Eq. (31)

$$\psi(s) = \sum_{\alpha=+,-}\sum_{n=-P}^{P} c_n^\alpha \psi_{\mu+n}^\alpha(s), \tag{75}$$

where μ is a given wavenumber taking the place of k in Eq. (31), c_n^α are Fourier coefficients, and the integer P is chosen to be sufficiently large so that the resulting eigenmode is well represented by the sum over n.

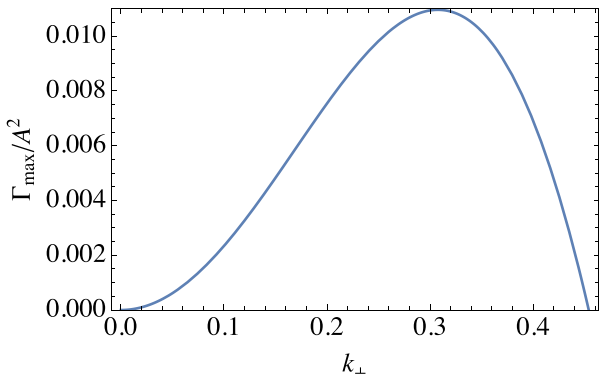

FIG. 7. Maximum growth rate $\Gamma_{\max}$ for the modulational instability in TG waves, plotted vs perpendicular wavenumber $k_\perp$.

Then, by using the inner product method outlined in Appendix A, we obtain a matrix eigenvalue problem for the frequency ω and the Fourier coefficients c_n^α

$$\omega c_n^\alpha = \sum_\beta \sum_{m=-P}^{P} \frac{\Lambda_{n,m}^{\alpha,\beta}}{E_{n+\mu}^\alpha} c_m^\beta, \tag{76}$$

where the Λ coefficients are given by Eq. (A3). The eigenvalues ω and eigenvectors c_n^α yield $2P+1$ eigenfrequencies and eigenfunctions that include Fourier harmonics with wavenumbers $k = n+\mu, n = -P, \ldots, P$. We repeat this evaluation for a set of μ values, $-1/2 \le \mu < 1/2$, in order to build up a set of eigenmodes. The values of μ beyond this range merely repeat the set of eigenmodes; the set is periodic in μ with a unit period since an integer added to μ can be removed by redefining n in the sum in Eq. (75) (assuming that P is sufficiently large so that the redefinition of the limits on the sum has no effect).

For large amplitude pump waves, the eigenmodes have many Fourier harmonics and P must be taken to be as large as possible. Eigenmodes dominated by wavenumbers approaching P are not very well converged. As a rule of thumb, eigenmodes with the $P/2$ lowest eigenfrequency magnitudes (since frequency is an increasing function of the wavenumber) are reasonably well converged. We take P values up to 60 and test for convergence in the eigenfrequencies as P is increased, keeping only those eigenfrequencies that exhibit good convergence (which always fall in the aforementioned lowest eigenfrequency grouping).

Calculated eigenfrequencies for a range of the low frequency well-converged modes are displayed in Fig. 8 vs μ, for a given pump amplitude A and $k_\perp = 3/2$, the same value as in Figs. 3–5. The lines visible in the figure are a superposition of the two dispersion relations ω_k^+ and ω_k^- shown in Figs. 3–5, shifted by nonlinear mode coupling effects. Since $k = \mu + n$ for some integer n, a given branch of the dispersion relation can be followed vs k out one side of the plot and into the other side, increasing or decreasing k by unity along that branch.

The locations of the four $k \neq 0$ degeneracies in Fig. 5 are shown as dots in Fig. 8, but with the k values shifted by an integer from those in Fig. 5 to values in the range $(-1/2, 1/2)$ using $k = n + \mu$. A careful

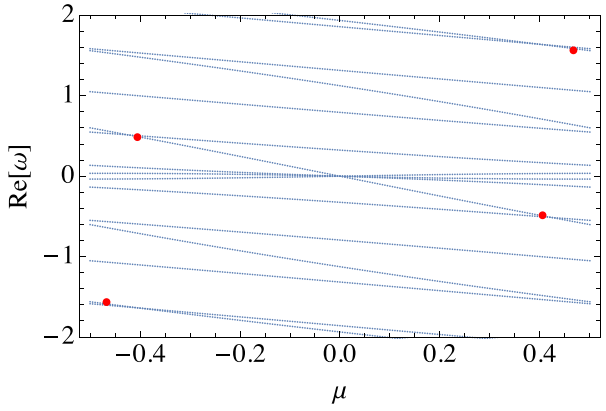

FIG. 8. Real part of the eigenmode frequencies vs wavenumber μ for pump amplitude $A = 0.1$ and $k_\perp = 3/2$. Dots are nontrivial degeneracy locations for $A \ll 1$ (see Figs. 5 and 6).

examination of the figure shows that the degeneracy locations are slightly changed by nonlinear effects. A scan of μ values performed around the predicted locations of degeneracies shows small instability regions, as expected from the theory. The imaginary part of ω is shown in Fig. 9 for $A = 0.05$, for wavenumbers near the $m = 2$ degeneracy, compared to the perturbation theory valid for small A. There is a slight shift in the location of the degeneracy compared to theory because second-order perturbation theory is not quite sufficient to predict the frequency shifts at this pump amplitude. However, the scaling with amplitude of the growth rate, the nonlinear shift in the degeneracy location, and the width of the degeneracy regions follow perturbation theory fairly well (at least, on a log scale), up to quite large pump amplitude (Fig. 10). The largest amplitude $A = 0.2$ in these plots corresponds to a pump wave density variation of over 100%. In these plots, the perturbation theory for the resonance locations and growth rates is calculated at small amplitudes A using Eqs. (65), (67), and (69), which employ Eqs. (A16), (A17), (A20), (A21), and (A22) for the matrix coefficients $\mathscr{L}$. We then simply extrapolated to larger amplitude using the expected lowest-order scaling with A for each plotted quantity. This seems to provide a better match to the numerical data than evaluating the perturbation theory for large A values, where perturbation expansions for frequency shifts and mode coupling are not valid.

For smaller $k_\perp$ values below $k_\perp = \sqrt{(\sqrt{5}-1)/6}$, a modulational instability is predicted near $|k| = 1$, which corresponds to $\mu = 0$. We have observed this instability in the numerical evaluation of the eigenmodes. In Fig. 11, we plot the imaginary part of the mode frequency compared to the theory of Eq. (74) for several pump wave amplitudes and for $k_\perp = 0.2$. The numerically determined growth rate agrees well with the perturbation theory, even for fairly large amplitude waves (the maximum possible amplitude at this $k_\perp$ value is roughly $A = 0.4$; see Fig. 2).

IV. DISCUSSION

In this paper, we have extended the analysis of Ref. 33 for the stability of nonlinear TG traveling waves to arbitrary wavenumber daughter waves. The new analysis shows that, while the pump waves are stable to three-wave processes, they can be unstable to four-wave and higher order processes over several narrow wavenumber bands, whose locations and widths are determined by wave degeneracies that depend on the amplitude of the pump and the perpendicular wavenumber. A long-wavelength 4-wave modulational instability was also described, similar to the instabilities studied in finite-amplitude water waves. Analytic expressions for the instability growth rates, valid at small pump wave amplitude, were compared to numerical evaluations, with good agreement found over applicable amplitude ranges.

Experiments on TG traveling waves in periodic boundary conditions have not yet been carried out, but such experiments could be done on systems such as the toroidal non-neutral plasma trap at Lawrence University,[41] where the plasma can be confined in a torus. Other experiments have observed the instability of nonlinear TG standing waves,[29] with growth rates far larger than those predicted here for traveling waves, or those predicted in Ref. 33 for standing waves. These experiments point to a kinetic instability mechanism caused by particles trapped in the potential wells of the pump wave.[30]

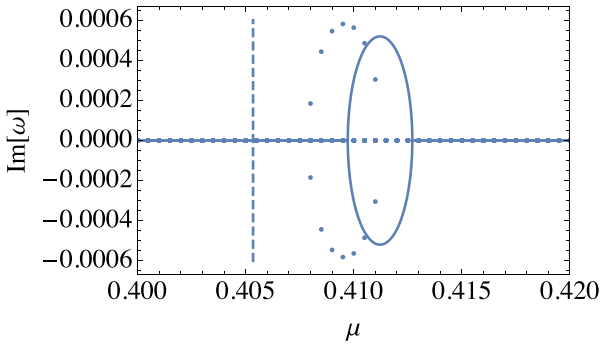

FIG. 9. Imaginary part of the eigenmode frequency plotted for a set of μ values near the $m = 2$ degeneracy, for pump amplitude $A = 0.05$ and $k_\perp = 3/2$. The solid line is perturbation theory, Eq. (68). The vertical dashed line is the $A \ll 1$ $m = 2$ degeneracy location (second dot from the right in Fig. 8).

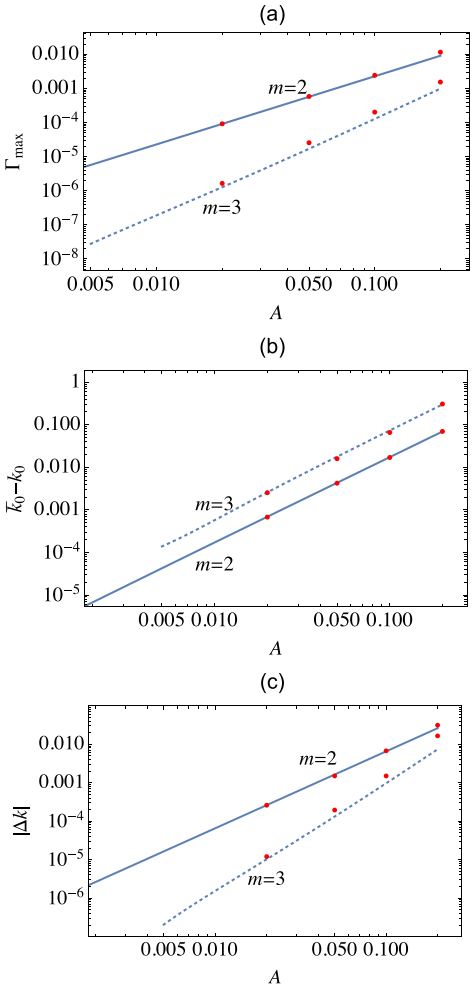

FIG. 10. (a) The maximum growth rate Γ_{max}, (b) shift in the degeneracy location $\bar{k}_0 - k_0$, and (c) width Δk of the instability region for both the $m = 2$ and $m = 3$ degeneracies for $k_\perp = 3/2$, plotted vs pump wave amplitude A. Lines are perturbation theory given by Eqs. (65), (67), and (69), extrapolated to large amplitude, and dots are from numerical evaluations.

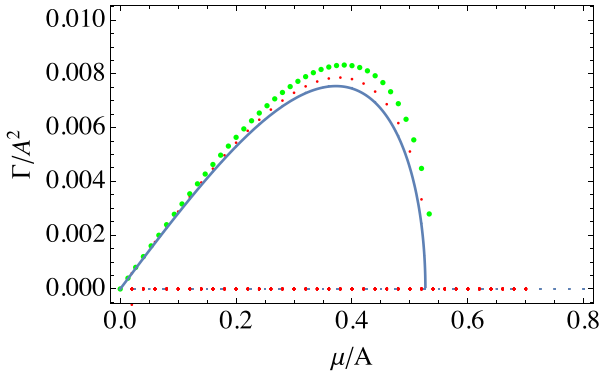

FIG. 11. Growth rate for the modulational instability vs wavenumber, each scaled by amplitude according to perturbation theory, for three amplitudes: $A = 0.05, 0.2, 0.3$ and for $k_\perp = 0.2$. The solid line is perturbation theory given by Eq. (74) with $\kappa = \mu/A$ and $\Gamma = A^2 \mathrm{Im}[\Delta\omega]$. Data for larger amplitude give slightly larger growth rates. The $A = 0.05$ numerical results cannot be distinguished from the theory curve.

Work on this kinetic mechanism is ongoing and will be reported on in the following paper.[42]

ACKNOWLEDGMENTS

The author thanks Dr. Matt Affolter and Professor T. O'Neil for useful discussions. This work was supported by U.S. DOE Grant No. DE-SC0018236 and NSF Grant No. PHY-1805764.

APPENDIX A: NONLINEAR COUPLING COEFFICIENTS

In this Appendix, we evaluate the nonlinear coupling coefficients in Eq. (63) for general $m > 1$. For higher-order degenerate perturbation theory applied to a resonance of the form $\omega_k^\alpha = \omega_{k+m}^\beta \equiv \omega_0$, $m > 1$, we cannot ignore the $\Delta\psi$ term appearing in Eq. (46). Instead, we express the eigenmode as

$$\psi(s) = \sum_{\bar\beta=+,-} \sum_{\bar n=-1}^{m+1} c_{\bar n}^{\bar\beta} \psi_{k+\bar n\bar\beta}(s), \tag{A1}$$

where the coefficients $c_0^\alpha \equiv C_1 = O(1)$ and $c_m^\beta \equiv C_2 = O(1)$, and all of the other coefficients are of order $A^p, p \geq 1$. The sum over $\bar n$ only needs to run from -1 to $m+1$ because only these waves are required to obtain the lowest nontrivial order for the matrix-coefficients given in Eq. (63). Substituting this expression for ψ into the eigenmode equation, Eq. (27), and taking an inner product with respect to one of the zeroth-order waves $\psi_{k+n}^{\bar\alpha}$ [using the zeroth-order inner product, Eq. (53)], yields the following matrix equation for the coefficients:

$$\omega E_{k+n}^{\bar\alpha} c_n^{\bar\alpha} = \sum_{\bar\beta=+,-} \sum_{\bar n=-1}^{m+1} \Lambda_{n,\bar n}^{\bar\alpha,\bar\beta} c_{\bar n}^{\bar\beta}, \tag{A2}$$

where $\Lambda_{n,\bar n}^{\bar\alpha,\bar\beta} = -i[\psi_{k+n}^{\bar\alpha}, \hat L \psi_{k+\bar n\bar\beta}]_0$. Using Eqs. (27), (28), (53), (8), (10), (11), and (12), this matrix coefficient can be expressed in terms of the Fourier coefficients of the pump wave

$$\Lambda_{n,\bar n}^{\bar\alpha,\bar\beta} = \frac{\omega_{k+n}^{\bar\alpha}}{4}\left[u_{k+n}^2 \delta_{n,\bar n} + V_{n-\bar n}\left(\bar\alpha u_{k+n} + \bar\beta u_{k+\bar n}\right) + \bar\alpha\bar\beta N_{n-\bar n} u_{k+n} u_{k+\bar n}\right], \tag{A3}$$

where we again employ the notation that multiplication by $\bar\alpha = +$ or $-$ means multiplication by $+1$ or -1, respectively, and similarly for $\bar\beta$.

In our analysis of the solution to this problem, it is important to note that, thanks to Eq. (17), the Λ coefficients are ordered in A according to $\Lambda_{n,\bar n}^{\bar\alpha,\bar\beta} = O(A^{|n-\bar n|})$. We explicitly account for the ordering by writing the coefficients as

$$\Lambda_{n,\bar n}^{\bar\alpha,\bar\beta} = A^{|n-\bar n|} \omega_{k+n}^{\bar\alpha} \lambda_{n,\bar n}^{\bar\alpha,\bar\beta}, \tag{A4}$$

where the coefficients $\lambda_{n,\bar n}^{\bar\alpha,\bar\beta}$ are order unity and are symmetric under interchange of the subscripts and superscripts: $\lambda_{n,\bar n}^{\bar\alpha,\bar\beta} = \lambda_{\bar n,n}^{\bar\beta,\bar\alpha}$.

Also, for $\bar n = n$, the matrix coefficient simplifies

$$\Lambda_{n,n}^{\bar\alpha,\bar\beta} = \omega_{k+n\bar\alpha} \begin{cases} E_{k+n}^{\bar\alpha} - \bar\alpha u_{k+n}(u' - u_1)/2, & \bar\alpha = \bar\beta \\ 0, & \bar\alpha \neq \bar\beta. \end{cases} \tag{A5}$$

The term $u' - u_1 \equiv A^2 \Delta u$ represents the nonlinear shift in the speed of the pump wave, and is $O(A^2)$, given by Eq. (15).

There are two equations from the set of $2m+6$ equations encoded in Eq. (A2) which we will reduce to the two-by-two-form of Eq. (63): the $\{n, \bar\alpha\} = \{0, \alpha\}$ equation and the $\{n, \bar\alpha\} = \{m, \beta\}$ equation. These two equations take the forms [using Eqs. (A4) and (A5)]

$$\left[E_k^\alpha(\omega - \omega_k^\alpha) + \alpha\omega_k^\alpha u_k \Delta u A^2/2\right] C_1 = A^m \omega_k^\alpha \lambda_{0,m}^{\alpha,\beta} C_2 + \sum_{\substack{\{\bar n,\bar\beta\} \\ \bar n \neq 0 \\ \{\bar n,\bar\beta\} \neq \{m,\beta\}}} \omega_k^\alpha A^{|\bar n|} \lambda_{0,\bar n}^{\alpha,\bar\beta} c_{\bar n}^{\bar\beta}, \tag{A6}$$

$$\left[E_{k+m}^\beta\left(\omega - \omega_{k+m}^\beta\right) + \beta\omega_{k+m}^\beta u_{k+m} \Delta u A^2/2\right] C_2 = A^m \omega_{k+m}^\beta \lambda_{m,0}^{\beta,\alpha} C_1 + \sum_{\substack{\{\bar n,\bar\beta\} \\ \{\bar n,\bar\beta\} \neq \{0,\alpha\} \\ \bar n \neq m}} \omega_{k+m}^\beta A^{|\bar n - m|} \lambda_{m,\bar n}^{\beta,\bar\beta} c_{\bar n}^{\bar\beta}. \tag{A7}$$

Here, we already begin to see the general form of the coupling given by Eq. (63). There is a direct coupling between C_1 and C_2 of order A^m, arising from the mth Fourier coefficients of the pump (since $\lambda_{m,0}^{\bar\beta,\bar\alpha}$ is proportional to a linear combination of V_m and N_m), and this coupling is symmetric on resonance, due to the symmetry of the λ coefficients. There are also diagonal nonlinear frequency shift terms of order A^2, arising from the nonlinear shift Δu in the pump wave speed.

The complete calculation of the nonlinear coupling coefficients in Eq. (63) requires the solution of the other $2m+4$ equations in Eq. (A2) for the small coefficients $c_{\bar n}^{\bar\beta}$ in terms of C_1 and C_2. The solution for these coefficients can be broken into two parts, with the following lowest-order expansion in A:

$$c_{\bar n}^{\bar\beta} = A^{|m-|m-\bar n||} g_{\bar n}^{\bar\beta} C_1 + A^{|m-|\bar n||} h_{\bar n}^{\bar\beta} C_2, \tag{A8}$$

where g and h are of order unity in A, except for the g_0 and h_m terms. We find that $g_0^{\alpha^\dagger} = O(A)$. Similarly, $h_m^{\beta^\dagger} = O(A)$. This ordering implies that these terms can be neglected, so that neither $c_0^{\alpha^\dagger}$ nor $c_m^{\beta^\dagger}$ are required in Eqs. (A6) or (A7). Thus, we can neglect both the $\bar{n} = 0$ and $\bar{n} = m$ terms in the sums, and we may take $g_0^{\alpha^\dagger} = h_m^{\beta^\dagger} = 0$ in Eq. (A8). The ordering provides the following forms for the matrix elements in Eq. (63). The $O(A^2)$ frequency shift terms are

$$\mathscr{L}_k^\alpha = -\alpha\omega_k^\alpha u_k \Delta u/2 + \omega_k^\alpha \sum_{\bar{\alpha}} \left(g_{-1}^{\bar{\alpha}} \lambda_{0,-1}^{\alpha,\bar{\alpha}} + g_1^{\bar{\alpha}} \lambda_{0,1}^{\alpha,\bar{\alpha}} \right), \tag{A9}$$

$$\mathscr{L}_{k+m}^\beta = -\beta\omega_{k+m}^\beta u_{k+m} \Delta u/2 + \omega_{k+m}^\beta \sum_{\bar{\alpha}} \left(h_{m-1}^{\bar{\alpha}} \lambda_{m,m-1}^{\beta,\bar{\alpha}} + h_{m+1}^{\bar{\alpha}} \lambda_{m,m+1}^{\beta,\bar{\alpha}} \right), \tag{A10}$$

and the $O(A^m)$ off diagonal elements are

$$\mathscr{L}_{k,k+m}^{\alpha,\beta} = \omega_k^\alpha \lambda_{0,m}^{\alpha,\beta} + \omega_k^\alpha \sum_{\bar{\alpha}} \sum_{n=1}^{m-1} h_n^{\bar{\alpha}} \lambda_{0,n}^{\alpha,\bar{\alpha}}, \tag{A11}$$

$$\mathscr{L}_{k+m,k}^{\beta,\alpha} = \omega_{k+m}^\beta \lambda_{m,0}^{\beta,\alpha} + \omega_{k+m}^\beta \sum_{\bar{\alpha}} \sum_{n=1}^{m-1} g_n^{\bar{\alpha}} \lambda_{m,n}^{\beta,\bar{\alpha}}. \tag{A12}$$

For $m = 1$, the sums do not enter and the off diagonal coefficients can be seen to agree with the off diagonal terms in Eq. (56), using Eqs. (A4), (A3), (10), and (18).

It is easy to solve for the g and h coefficients in Eqs. (A9) and (A10), since these coefficients enter only at $O(A)$ in Eq. (A8). Solving Eq. (A2) for $g_{\pm 1}^{\bar{\alpha}}$ and $h_{m\pm 1}^{\bar{\alpha}}$ yields, to the lowest order

$$g_n^{\bar{\alpha}} = \frac{\omega_{k+n}^{\bar{\alpha}} \lambda_{n,0}^{\bar{\alpha},\alpha}}{d_n^{\bar{\alpha}}}, \quad n = \pm 1, \tag{A13}$$

$$h_n^{\bar{\alpha}} = \frac{\omega_{k+n}^{\bar{\alpha}} \lambda_{n,m}^{\bar{\alpha},\beta}}{d_n^{\bar{\alpha}}}, \quad n = m \pm 1, \tag{A14}$$

where

$$d_n^{\bar{\alpha}} = E_{k+n}^{\bar{\alpha}} \omega - \Lambda_{n,n}^{\bar{\alpha},\bar{\alpha}} \tag{A15}$$

is the diagonal coefficient in the *nth* equation. When these expressions are used to determine the frequency shift via Eqs. (A9) and (A10), we obtain

$$\mathscr{L}_k^\alpha = -\alpha\omega_k^\alpha u_k \Delta u/2 + \omega_k^\alpha \sum\nolimits_{\bar{\alpha}} \left[\omega_{k-1}^{\bar{\alpha}} \frac{\left(\lambda_{0,-1}^{\alpha,\bar{\alpha}}\right)^2}{d_{-1}^{\bar{\alpha}}} + \omega_{k+1}^{\bar{\alpha}} \frac{\left(\lambda_{0,1}^{\alpha,\bar{\alpha}}\right)^2}{d_1^{\bar{\alpha}}} \right], \tag{A16}$$

$$\mathscr{L}_{k+m}^\beta = -\beta\omega_{k+m}^\beta u_{k+m} \Delta u/2 + \omega_{k+m}^\beta \sum_{\bar{\alpha}} \left[\omega_{k+m-1}^{\bar{\alpha}} \frac{\left(\lambda_{m,m-1}^{\beta,\bar{\alpha}}\right)^2}{d_{m-1}^{\bar{\alpha}}} + \omega_{k+m+1}^{\bar{\alpha}} \frac{\left(\lambda_{m,m+1}^{\beta,\bar{\alpha}}\right)^2}{d_{m+1}^{\bar{\alpha}}} \right], \tag{A17}$$

where we have used the symmetry of the λ coefficients under the exchange of indices.

The other g and h coefficients required in Eqs. (A11) and (A12) can also be determined by solving Eq. (A2) for $\bar{n} = 1, \ldots, m-1$, noting that for each $\bar{n}$ value that part of the equation proportional to C_1 can be solved independently of the part proportional to C_2. The C_1 part yields the $g_{\bar{n}}^{\bar{\alpha}}$ coefficient in terms of coefficients with smaller $\bar{n}$ and is of order $A^{\bar{n}}$. The C_2 part yields the $h_{\bar{n}}^{\bar{\alpha}}$ coefficient in terms of coefficients with larger $\bar{n}$ and is of order $A^{m-\bar{n}}$. The solutions are given below, enabling a recursive construction of the g and h coefficients

$$g_n^{\bar{\alpha}} = \omega_{k+n}^{\bar{\alpha}} \frac{\lambda_{n,0}^{\bar{\alpha},\alpha} + \sum_{\bar{\beta}} \sum_{\bar{n}=1}^{n-1} \lambda_{n,\bar{n}}^{\bar{\alpha},\bar{\beta}} g_{\bar{n}}^{\bar{\beta}}}{d_n^{\bar{\alpha}}}, \quad n = 1, \ldots, m-1, \tag{A18}$$

$$h_n^{\bar{\alpha}} = \omega_{k+n}^{\bar{\alpha}} \frac{\lambda_{n,m}^{\bar{\alpha},\beta} + \sum_{\bar{\beta}} \sum_{\bar{n}=n+1}^{m-1} \lambda_{n,\bar{n}}^{\bar{\alpha},\bar{\beta}} h_{\bar{n}}^{\bar{\beta}}}{d_n^{\bar{\alpha}}}, \quad n = m-1, \ldots, 1. \tag{A19}$$

For example, for $m = 2$, only the $n = 1$ terms are needed, with forms already given explicitly in Eqs. (A13) and (A14). When they are applied to Eqs. (A11) and (A12), we obtain the following form for the off diagonal coupling coefficients in the reduced matrix:

$$\mathscr{L}_{k,k+2}^{\alpha,\beta} = \omega_k^\alpha \lambda_{0,2}^{\alpha,\beta} + \omega_k^\alpha \sum_{\bar{\alpha}} \omega_{k+1}^{\bar{\alpha}} \frac{\lambda_{0,1}^{\alpha,\bar{\alpha}} \lambda_{1,2}^{\bar{\alpha},\beta}}{d_1^{\bar{\alpha}}}, \tag{A20}$$

$$\mathscr{L}_{k+2,k}^{\beta,\alpha} = \omega_{k+2}^\beta \lambda_{2,0}^{\beta,\alpha} + \omega_{k+2}^\beta \sum_{\bar{\alpha}} \omega_{k+1}^{\bar{\alpha}} \frac{\lambda_{2,1}^{\beta,\bar{\alpha}} \lambda_{1,0}^{\bar{\alpha},\alpha}}{d_1^{\bar{\alpha}}}. \tag{A21}$$

On resonance, where $\omega_k^\alpha = \omega_{k+2}^\beta$, $\mathscr{L}_{k+2,k}$ and $\mathscr{L}_{k,k+2}$ are identical due to the symmetry of the λ coefficients.

For $m = 3$, the coupling coefficients are given by

$$\frac{\mathscr{L}_{k,k+3}^{\alpha,\beta}}{\omega_k^\alpha} = \frac{\mathscr{L}_{k+3,k}^{\beta,\alpha}}{\omega_{k+3}^\beta} = \lambda_{0,3}^{\alpha,\beta} + \sum_{\bar{\alpha}} \frac{\omega_{k+1}^{\bar{\alpha}}}{d_1^{\bar{\alpha}}} \lambda_{0,1}^{\alpha,\bar{\alpha}} \lambda_{1,3}^{\bar{\alpha},\beta} + \sum_{\bar{\alpha}} \frac{\omega_{k+2}^{\bar{\alpha}}}{d_2^{\bar{\alpha}}} \lambda_{0,2}^{\alpha,\bar{\alpha}} \lambda_{2,3}^{\bar{\alpha},\beta} + \sum_{\bar{\alpha},\bar{\beta}} \frac{\omega_{k+1}^{\bar{\alpha}} \omega_{k+2}^{\bar{\beta}}}{d_1^{\bar{\alpha}} d_2^{\bar{\beta}}} \lambda_{0,1}^{\alpha,\bar{\alpha}} \lambda_{1,2}^{\bar{\alpha},\bar{\beta}} \lambda_{2,3}^{\bar{\beta},\beta}. \tag{A22}$$

For larger m, the coupling coefficients continue this pattern, summing over every combination of λ coefficients that couple mode 0 to mode m.

Note that these coefficients depend implicitly on the eigenfrequency ω, through the d coefficient [see Eq. (A15)]. The problem is made tractable by taking for ω the zeroth-order value at degeneracy, $\omega = \omega_0$. This is sufficient to obtain the lowest order forms for the frequency shifts and off-diagonal mode coupling coefficients.

We now return to the special case of the modulational instability and evaluate the matrix coefficients in Eq. (63). Recall that for this $m = 2$ degeneracy, the daughter waves have wavenumbers $k = -1 + \Delta k$ and $k = 1 + \Delta k$ and both are on the + branch of the dispersion relation. The mode coupling coefficients, the daughter wave energies, and their frequencies all vanish at the $m = 2$ degeneracy point $k = -1$, so there is mode coupling and instability only for $\Delta k \neq 0$. Since all terms vanish at $\Delta k = 0$ in Eq. (63), we Taylor-expand each matrix coefficient in small Δk. Writing $\Delta k = A\kappa$ and $\omega = Av_1^+\kappa + A^2\Delta\omega$ [where v_1^+ is the daughter wave group velocity; see Eq. (60)], the reduced matrix equation (63) has the form

$$\begin{pmatrix} \kappa\epsilon\Delta\omega + \kappa(a - b\kappa^2) & \kappa a \\ \kappa a & -\kappa\epsilon\Delta\omega + \kappa(a - b\kappa^2) \end{pmatrix} \cdot \begin{pmatrix} C_1 \\ C_2 \end{pmatrix} = 0, \tag{A23}$$

where we have divided a factor of A^3 from the matrix. Dividing out a factor of κ then yields Eq. (70). The coefficient ϵ is the first-order Taylor expansion coefficient of the first daughter wave energy E_k^+

$$\epsilon(k_\perp) = \partial E_k^+/\partial k|_{k=-1} = \frac{1}{2\left(1+k_\perp^2\right)^2}, \tag{A24}$$

where we used Eqs. (43) and (14). Thanks to symmetry about $k=0$, the second daughter wave energy E_{k+2}^+ has a Taylor expansion about $k=-1$ of the opposite sign.

The dispersive term b arises from the Taylor expansion of ω_k^+ to second-order in Δk, multiplied by the Taylor expansion of E_k

$$b = (\epsilon/2)\partial^2\omega_k^+/\partial k^2|_{k=-1} = \frac{3k_\perp^2}{4\left(1+k_\perp^2\right)^{9/2}}, \tag{A25}$$

where we used Eqs. (41) and (14). The Taylor expansion for the other daughter wave at $k=1$ leads to the same coefficient, thanks to symmetry about $k=0$.

Here, we should pause to note that the first-order term in the Taylor expansion of ω_k^+ has already been accounted for through our choice of the form of the eigenfrequency, $\omega = v_1^+\Delta k + A^2\Delta\omega$. The first-order Taylor expansion of ω_k^+ at $k=-1$ yields $v_{-1}^+\Delta k$, which cancels with the first order term in the eigenfrequency, $v_1^+\Delta k$. (Note that $v_{-1}^+ = v_1^+$ by symmetry.) Also, thanks to the symmetry about $k=0$, this cancelation occurs for the second daughter wave as well.

The mode coupling term a can be evaluated by Taylor-expansion to first order in Δk of either Eqs. (A16), (A17), and (A20) or (A21); all give the same result. For example, comparing Eq. (63) with Eq. (A23), we can write $a = -\partial\mathscr{L}_k^\alpha/\partial k|_{k=-1}$. Since Eq. (A16) shows that, for $\alpha=\beta=+$, $\mathscr{L}_k^\alpha$ is proportional to ω_k^+, which vanishes at $k=\pm1$, we obtain

$$a = v_{-1}^+\left\{u_1\frac{\Delta u}{2} - \sum_{\bar\alpha}\left[\omega_{k-1}^{\bar\alpha}\frac{\left(\lambda_{0,-1}^{+,\bar\alpha}\right)^2}{d_{-1}^{\bar\alpha}} + \omega_{k+1}^{\bar\alpha}\frac{\left(\lambda_{0,1}^{+,\bar\alpha}\right)^2}{d_1^{\bar\alpha}}\right]_{k=-1}\right\}. \tag{A26}$$

L'Hôpital's rule and the first-order form for the eigenfrequency, $\omega = \Delta k\, v_1^+$, must be used to evaluate $\omega_{k+1}^{\bar\alpha}/d_1^{\bar\alpha}|_{k=-1}$

$$\frac{\omega_{k+1}^{\bar\alpha}}{d_1^{\bar\alpha}}|_{k\to-1} = \frac{2(\bar\alpha u_0 - u_1)}{u_0(u_0 - \bar\alpha u_1)\left(u_1 + v_1^+ - \bar\alpha u_0\right)}. \tag{A27}$$

For $d_{-1}^{\bar\alpha}$, it is sufficient to simply take $\omega=0$, yielding $d_{-1}^{\bar\alpha}|_{k=-1} = -4\omega_{-2}^{\bar\alpha}E_{-2}^{\bar\alpha}$ to the lowest order in A. Applying these results to Eq. (A26) along with the forms for the λ coefficients given by Eqs. (A4) and (A3), and the shift $\Delta u = (u' - u_1)/A^2 = 2 + 3k_\perp^2/4$ from Eq. (15), we obtain, after some algebra

$$a = \frac{k_\perp^2}{8\left(1+k_\perp^2\right)^{5/2}}\,\frac{1 - 3k_\perp^2 - 9k_\perp^4}{1 + 3k_\perp^2 + 3k_\perp^4}. \tag{A28}$$

REFERENCES

[1] T. B. Benjamin, "Instability of periodic wavetrains in nonlinear dispersive systems," Proc. R. Soc. A **299**, 59 (1967).
[2] T. B. Benjamin and J. E. Frier, "The disintegration of wave trains in deep water. Part 1. Theory," J. Fluid Mech. **27**, 417 (1967).
[3] N. Bottman and B. Deconinck, "KdV cnoidal waves are linearly stable," Discrete Contin. Dyn. Syst. **25**, 1163 (2009).
[4] G. B. Whitham, *Linear and Nonlinear Waves* (Wiley Interscience, New York, 1999).
[5] D. J. Kaup, "A higher-order water-wave equation and the method of solving it," Prog. Theor. Phys. **54**, 396 (1975).
[6] A. V. Mikhailov, *Integrability*, *Lecture Notes in Physics* Vol. 767 (Springer, Berlin, 2009).
[7] J. E. Feir, "Discussion: Some results from wave pulse experiments," Proc. Roy. Soc. A **299**, 54 (1967).
[8] G. B. Whitham, "A general approach to linear and non-linear dispersive waves using a Lagrangian," J. Fluid Mech. **22**, 273 (1965).
[9] G. B. Whitham, "Nonlinear dispersion of water waves," J. Fluid Mech. **27**, 399 (1967).
[10] M. S. Longuet-Higgins, "The instabilities of gravity waves of finite amplitude in deep water I. Superharmonics," Proc. R. Soc. A **360**, 471 (1978).
[11] M. S. Longuet-Higgins, "The instabilities of gravity waves of finite amplitude in deep water II. Subharmonics," Proc. R. Soc. A **360**, 489 (1978).
[12] R. Z. Sagdeev and A. A. Galeev, *Nonlinear Plasma Theory* (W. A. Benjamin, New York, 1969).
[13] R. C. Davidson, *Methods in Nonlinear Plasma Theory* (Academic Press, New York, 1972).
[14] P. K. Kaw, W. L. Kruer, C. S. Liu, and K. Nishikawa, *Advances in Plasmas Physics* (John Wiley Interscience, New York, 1976), Vol. 6.
[15] A. A. Galeev and V. N. Oraevskii, Sov. Phys. Dokl. **7**, 988 (1962).
[16] L. M. Kovrizhnykh and V. N. Tsytovich, Sov. Phys. Dokl. **9**, 913 (1965).
[17] M. Porkolab, S. Bernabei, W. M. Hooke, R. W. Motley, and T. Nagashima, Phys. Rev. Lett. **38**, 230 (1977).
[18] H. C. Bandulet, C. Labaune, K. Lewis, and S. Depierreux, Phys. Rev. Lett. **93**, 035002 (2004).
[19] C. Niemann, S. H. Glenzer, J. Knight, L. Divol, E. A. Williams, G. Gregori, B. I. Cohen, C. Constantin, D. H. Froula, D. S. Montgomery, and R. P. Johnson, Phys. Rev. Lett. **93**, 045004 (2004).
[20] A. Tenerani, M. Velli, and P. Hellinger, Astrophys. J. **851**, 99 (2017).
[21] M. G. Krein and V. A. Jakubbovic, *Four Papers on Ordinary Differential Equations* (American Mathematical Society, Providence RI, 1980).
[22] J. K. Moser, Mem. Am. Math. Soc. **81**, 1 (1968).
[23] F. R. S. Lord Rayleigh, "On the equilibrium of liquid conducting masses charged with electricity," London, Edinburg Dublin Philos. Mag. J. Sci. **14**(87), 184 (1882).
[24] I. B. Bernstein, E. A. Frieman, M. D. Kruskal, and R. M. Kulsrud, "An energy principle for hydromagnetic stability problems," Proc. R. Soc. London, Ser. A. **244**, 17 (1958).
[25] E. Frieman and M. Rotenberg, "On hydromagnetic stability of stationary equilibria," Rev. Mod. Phys. **32**, 898 (1960).
[26] P. J. Morrison, "Hamiltonian description of the ideal fluid," Rev. Mod. Phys. **70**, 467 (1998).
[27] B. Deconinck and J. N. Kutz, "Computing spectra of linear operators using the Floquet-Fourier-Hill method," J. Comput. Phys. **219**, 296 (2006).
[28] H. Higaki, Plasma Phys. Controlled Fusion **39**, 1793 (1997).
[29] M. Affolter, F. Anderegg, D. H. E. Dubin, F. Valentini, and C. F. Driscoll, "Trapped particle effects in the parametric instability of near-acoustic waves," Phys. Rev. Lett. **121**, 235004 (2018).
[30] D. H. E. Dubin, Phys. Rev. Lett. **121**, 015001 (2018).
[31] A. W. Trivelpiece and R. W. Gould, J. Appl. Phys. **30**, 1784 (1959).
[32] J. H. Malmberg and C. B. Wharton, Phys. Rev. Lett. **17**, 175 (1966).
[33] D. H. E. Dubin and A. Ashourvan, Phys. Plasmas **22**, 102102 (2015).
[34] W. M. Mannheimer, Phys. Fluids **12**, 2426 (1969).
[35] J. R. Danielson, D. H. E. Dubin, R. G. Greaves, and C. M. Surko, Rev. Mod. Phys. **87**, 247 (2015).
[36] L. Rayleigh, "Investigation of the character of the equilibrium of an incompressible heavy fluid of variable density," Proc. London Math. Soc. **s1–14**, 170

(1883); G. I. Taylor, "The instability of liquid surfaces when accelerated in a direction perpendicular to their planes," Proc. R. Soc., A **201**, 192 (1950).
[37]L. Landau and E. M. Lifshitz, *Mechanics* (Pergamon Press, Oxford, 1969).
[38]G. Floquet, "Sur les equations differentielles lineaires a coefficients periodiques," Ann. Sci. Ec. Norm. Super. **12**, 47 (1883).
[39]A. Mostafazadeh, J. Math. Phys. **43**, 205 (2002).
[40]T. Ya. Azizov and I. S. Iokhvidov, *Linear Operators in Spaces With an Indefinite Metric* (John Wiley and Sons, Chichester, 1989).
[41]M. R. Stoneking, J. P. Marler, B. N. Ha, and J. Smoniewski, "Experimental realization of nearly steady-state toroidal electron plasmas," Phys. Plasmas **16**, 055708 (2009).
[42]D. H. E. Dubin, "Instability of nonlinear Trivelpiece-Gould waves II: Weakly-trapped particles," Phys. Plasmas (2019).